NACA RM E53A30

NACA

RESEARCH MEMORANDUM

EFFECT OF DIFFUSER DESIGN, DIFFUSER-EXIT VELOCITY PROFILE AND FUEL DISTRIBUTION ON ALTITUDE PERFORMANCE OF SEVERAL AFTERBURNER CONFIGURATIONS

By E. William Conrad, Frederick W. Schulze, and Karl H. Usow

Lewis Flight Propulsion Laboratory
Cleveland, Ohio

NATIONAL ADVISORY COMMITTEE
FOR AERONAUTICS
WASHINGTON

July 9, 1953
Declassified January 20, 1958

NATIONAL ADVISORY COMMITTEE FOR AERONAUTICS

RESEARCH MEMORANDUM

EFFECT OF DIFFUSER DESIGN, DIFFUSER-EXIT VELOCITY PROFILE, AND FUEL DISTRIBUTION ON ALTITUDE PERFORMANCE OF SEVERAL AFTERBURNER CONFIGURATIONS

By E. William Conrad, Frederick W. Schulze, and Karl H. Usow

SUMMARY

An investigation was conducted in the Lewis altitude wind tunnel to improve the altitude performance and operational characteristics of an afterburner primarily by modifying the diffuser-exit velocity profile by changes in diffuser design and by changing the fuel distribution and the flame holder. Twenty configurations consisting of combinations of six diffuser geometries, six flame-holder types, and twelve fuel systems were investigated. Data were obtained over a range of afterburner fuel-air ratios at diffuser-inlet total pressures from 2750 to 620 pounds per square foot.

Variations of the velocity profile produced the greatest effect on afterburner combustion efficiency at the pressure level of 620 pounds per square foot. A peak combustion efficiency of only 0.54 was obtained with a velocity profile that varied from 630 feet per second near the outer flame-holder gutter to zero velocity or reverse flow near the center line of the burner. In contrast, a peak efficiency of 0.90 was possible with a velocity which varied from a maximum value of 590 feet per second near the shell to about 430 feet per second at the center line. The latter profile provided a velocity as low as 220 feet per second near the flame-holder gutters.

Changes in fuel distribution affected the fuel-air ratio at which peak combustion efficiency occurred as well as the efficiency level. At the pressure level of 2750 pounds per square foot, a uniform distribution is desired at the high fuel-air ratio. Increase in fuel-orifice size to permit operation without excessive fuel-pump pressures at low altitudes impaired the performance at high altitudes.

Screeching combustion, which was most prevalent at low altitudes and medium-to-high fuel-air ratios, imposed a restriction on the operable range of a number of configurations. The configurations incorporating a diffuser which produced a very high velocity near the flame-holder gutter were most prone to screech.

INTRODUCTION

An investigation was conducted in the NACA Lewis altitude wind tunnel to improve the altitude performance and operational characteristics of a production afterburner. Early in the investigation it was found (ref. 1) that improvement in the velocity profile leaving the afterburner diffuser was necessary to the attainment of better performance at high altitudes. Accordingly, methods of altering the diffuser-outlet (burner-inlet) velocity profile by changes in diffuser design were studied, and the resulting effects on afterburner performance were determined. Six different diffuser designs were used during the study reported herein.

The merit of each of the diffuser configurations is considered in terms of the outlet velocity profile produced, the total-pressure loss incurred, and the resulting effects of the velocity profile on afterburner combustion efficiency. Where a diffuser configuration produced either low pressure losses or a uniform velocity pattern, numerous changes to the fuel system or flame holder were made in an effort to optimize the performance. Little or no effort was expended in such changes, however, when the pressure losses were high or the profile nonuniform. The effects of these changes on both performance and operational characteristics are also discussed, particularly with reference to screeching combustion which was encountered under certain operating conditions with most of the configurations studied.

Data were obtained at limiting turbine-outlet temperature over a range of afterburner fuel-air ratios at altitudes from 10,000 to 45,000 feet, corresponding to diffuser-inlet total pressures from 2750 to 620 pounds per square foot absolute.

APPARATUS

Engine

The engine used in this investigation was designated the prototype J40-WE-8 turbojet engine, which has a sea-level static rating without afterburning of 7500 pounds thrust at an engine speed of 7260 rpm. At this rating, the turbine-inlet gas temperature is 1425° F and the engine air flow is approximately 142 pounds per second.

Main components of the engine include an 11-stage axial-flow compressor, a single-annulus basket-type combustor, a two-stage turbine, a diffuser assembly, a 37-inch-diameter afterburner combustion chamber with cooling shroud, a clamshell-type variable-area exhaust nozzle, and an electronic control.

During afterburner operation, the electronic control varied engine fuel flow and exhaust-nozzle area to maintain engine speed and turbine-outlet temperature. The turbine-outlet (diffuser-inlet) temperature was sensed by nine chromel-alumel thermocouples located downstream of the turbine. During afterburner operation, the exhaust nozzle was actuated by the control to maintain a given diffuser-inlet temperature over the full range of afterburner fuel-air ratios. The exhaust-nozzle area was 624 square inches when fully open.

Over-all length of the engine is approximately 284 inches, maximum height is $45\frac{1}{2}$ inches, maximum width is $42\frac{1}{4}$ inches, and the total weight is approximately 3560 pounds.

Installation

The engine was mounted on a wing section that spanned the 20-foot test section of the altitude wind tunnel, as shown in figure 1. Engine-inlet total pressures corresponding to altitude flight conditions were obtained by introducing dry refrigerated air from the tunnel make-up air system through a duct to the engine inlet. A slip joint with a frictionless seal used in the duct made possible the measurement of thrust and installation drag with the tunnel scales. Air was throttled from approximately sea-level pressure to the desired pressure at the engine inlet, while the static pressure in the tunnel test section was maintained to correspond to the desired altitude pressure.

Instrumentation

Instrumentation for measuring pressures and temperatures was installed at several stations throughout the engine and afterburner as indicated in figure 2. Total pressures and temperatures at the turbine outlet were obtained 3 inches downstream of the turbine outlet from four rakes having five total-pressure tubes and six thermocouples each. Pressures at the diffuser outlet were taken from a vertical survey made by 21 total-pressure tubes and two wall static-pressure taps located $42\frac{1}{2}$ inches downstream of the turbine outlet.

At a location $4\frac{1}{2}$ inches upstream of the exhaust-nozzle outlet, pressures were measured by 17 total-pressure and 6 static-pressure tubes in a vertical water-cooled rake which was mounted so that the rake drag could be measured by a pneumatic capsule. Screeching combustion was sensed by a pressure pickup mounted on the afterburner skin in the plane

of the flame holder. The pressure fluctuations were transmitted to a panoramic-sonic analyzer capable of recording frequency vibrations to 20,000 cycles per second.

AFTERBURNER DESIGNS

Afterburner shell. - A sketch of the afterburner shell showing pertinent dimensions is given in figure 3. This shell was common to all configurations investigated. Air to the cooling shroud was bled from the compressor outlet through a $3\frac{3}{8}$-inch line which had a manually controlled butterfly valve.

Diffusers. - The six diffuser designs used in the investigation are sketched in figure 4. Photographs of some of these diffusers are shown in figures 5 to 8. The blunt-end inner cone which is part of diffuser A is pictured in figure 5. This cone was also common to diffusers B and D. Diffuser B differed from A by the addition of an annular cascade assembly of five vanes which was supplied by the engine manufacturer. A view, looking downstream, of the assembly as mounted in the diffuser section is shown in figure 6. Diffuser C comprised a long inner cone and a ring of 30 vortex generators on the inner body immediately downstream of the turbine. These vortex generators were noncambered symmetrical airfoils of 2-inch chord and $\frac{1}{2}$-inch span, and were mounted alternately 10° and -10° to the gas-flow direction. Diffuser D was the same as B, except that the fourth and fifth deflector vanes were removed from the annular cascade assembly. Diffuser E, a view of which is shown in figure 7, incorporated the long inner cone of diffuser C and the second and third vanes from the annular cascade assembly. Diffuser F, shown in figure 8, was supplied by the engine manufacturer; the design of this diffuser was based on the work reported in reference 2. This diffuser incorporated a small effective expansion angle which minimized adverse pressure gradients in an effort to eliminate regions of flow separation which may be the cause in some cases of screeching combustion.

Flame holders. - The various flame holders used during this investigation are shown by the sketches and photographs of figure 9. Flame holder A is a conventional 2-V-gutter flame holder furnished by the engine manufacturer. Louvers were used in the leading edges of the gutters, and flame-stabilizing bars were used between the gutters and inside the inner gutter as shown in the photograph of figure 9(a). This flame holder blocked 41.3 percent of the cross-sectional area of the combustion chamber. The flame-holder blocked area is considered to be the projected area of the flame holder, including support struts and flame-stabilizing bars where used.

Flame holder B (fig. 9(b)) is a 2-V-gutter flame holder blocking 33.9 percent of the cross-sectional area. The gutters were staggered, and radial gutters were used to increase the perimeter of the flame surface. Flame holder C (fig. 9(c)) is the same as A, except that the center flame-stabilizing bars were replaced by a third gutter having three radial strut gutters. This change was intended to provide flame stabilization in the rather large open area in flame holder A. Blockage was 40.6 percent of the cross-sectional area of the combustion chamber.

Flame holder D (fig. 9(d)) is a 3-V-gutter flame holder blocking 40.5 percent of combustion-chamber area. The outer gutter was the same as the outer gutter of flame holder A, while the inner two gutters were corrugated.

Flame holder E, designed by the manufacturer for use with diffuser F, is shown installed in figure 8. This flame holder incorporated flame-stabilizing bars and blocked 21.4 percent of the afterburner cross-sectional area (does not include flame-seat area at rear of inner cone).

Flame holder F is the same as E, except that $\frac{1}{4}$-inch-high flat strips were welded to the trailing edge of all flame-holder surfaces. This flame holder blocked 25.6 percent of the cross-sectional area.

Fuel systems. - Fuel injection to the afterburner was accomplished with either a three-ring manifold, a five-ring manifold, or radial fuel-spray bars. Details of these three types of system showing the modifications made to them are given in figure 10. Changes to the fuel systems will be discussed in conjunction with the RESULTS AND DISCUSSION and OPERATIONAL CHARACTERISTICS.

Summary of configuration details. - Table I, which is a summary of configuration arrangements, shows how all the component parts described in the previous sections were assembled to produce the 20 individual configurations investigated. The extent to which certain variables were held constant while changes to another variable were made is also shown in the table. Letters A through F will denote the diffuser type used, while changes with a given diffuser type comprising a single configuration are denoted by numbers 1, 2, 3, and so forth.

PROCEDURE

The three simulated flight conditions at which performance data were obtained are shown in the following table:

Altitude, ft	Flight Mach number
10,000	0.18
35,000	.78
45,000	.18

Because of facility limitations, the data at altitudes of 10,000 and 45,000 feet could not be obtained at simulated flight Mach numbers above 0.18; also, the engine-inlet temperature could not be reduced below -20° F. Thus, the range of diffuser-inlet total pressures was from about 2750 pounds per square foot absolute at an altitude of 10,000 feet to about 620 pounds per square foot absolute at an altitude of 45,000 feet. Although this latter pressure is lower than the minimum given in the engine specifications (730 pounds per square foot), adequate performance at the lower pressure was desired to provide a "margin of safety." Data at the intermediate altitude were obtained to measure the performance at a flight speed within the normal flight envelope of most airplanes. Not all configurations were run at each of the three altitude conditions, but sufficient data were obtained in most cases to indicate the relative merit of each configuration.

About 2 to $2\frac{1}{2}$ percent of engine air flow was bled from the compressor outlet to cool the rear afterburner shell. Initial ignition of the afterburner fuel was accomplished with a "hot-streak" system of adding a quantity of fuel at the turbine inlet to provide a burst of flame through the turbine.

In many configurations, three fuel-flow-regulating systems were in use, which made possible the measurement of fuel pressures and flow to individual rings or bars. Variations in fuel distribution by varying throttle settings of the individual systems permitted a study of the effect of fuel distribution. At the intermediate flight condition the optimum performance was determined at a fuel-air ratio of 0.035. The fuel distribution thus determined was used at the higher and lower altitudes.

Data were obtained over a range of afterburner fuel-air ratios from the lean blow-out limit to a maximum value determined by either maximum exhaust-nozzle area, maximum allowable fuel pressure, rich blow-out, or screeching combustion.

Fuel conforming to specifications MIL-F-5624A (grade JP-4) was used throughout the investigation except for a brief investigation of operation with grade JP-3 fuel and a grade JP-3 fuel with tetraethyl lead additive.

RESULTS AND DISCUSSION

Average diffuser-inlet conditions. - Inasmuch as the diffuser-inlet total pressures and temperatures were not influenced by changes in the afterburner configuration, the data shown in figure 11 are representative of conditions obtained throughout the investigation. In accordance with a previously determined relation between turbine-inlet and turbine-outlet total temperatures, the outlet (diffuser-inlet) temperature was allowed to vary with flight conditions as shown in figure 11(a) from an average value of 1505° R at 10,000 feet altitude to 1640° R at 45,000 feet altitude. The diffuser-inlet total pressure, as shown in figure 11 (b), ranged from an average value of 620 pounds per square foot at 45,000 feet altitude to 2750 pounds per square foot at 10,000 feet altitude.

Diffuser characteristics. - Velocity distributions obtained from the survey at the exit of each of the diffusers are shown in figures 12 and 13, and values of total-pressure loss are presented in figure 14. For diffusers A to E the station of measurement was $42\frac{1}{2}$ inches downstream of turbine outlet, the area at the station being 2.16 times that of turbine outlet; for diffuser F, the station was 31 inches downstream of turbine outlet, the area at this station being 1.70 times that of turbine outlet. The velocity profiles of diffusers A and C are shown in figure 12(a). Diffuser A produced a velocity profile varying from 630 feet per second 12 inches from the center to zero velocity or reverse flow at the center. The existence of reverse-flow region was indicated by the fact that a total-pressure tube on the center-line pointing downstream indicated a higher pressure than a similar tube pointing upstream. This core of gas having a reverse flow was about 10 inches in diameter and appeared to be a result of flow separation from the blunt inner cone of diffuser A. Total-pressure loss for diffuser A was 0.043 of the diffuser-inlet total pressure (fig. 14).

Use of a long inner cone and a ring of vortex generators (based on ref. 3) in diffuser C did not eliminate separation from the inner body. A peak velocity of 660 feet per second existed about 9 inches from the center line, while the reverse-flow area in the center was 6 inches in diameter (fig. 12(a)). The pressure loss obtained with diffuser C was 0.047 of the diffuser-inlet total pressure, slightly higher than that of diffuser A (fig. 14).

The velocity profiles obtained with diffusers B, D, and E are compared in figure 12(b). Addition of the annular cascade assembly to the blunt inner cone to form diffuser B resulted in a considerably flattened velocity distribution compared with that produced by diffuser A and eliminated the reverse-flow regions in the center. Peak velocity was 590 feet per second, while center-line velocity was 435 feet per second.

Wakes appear to exist downstream of the vanes. Total-pressure loss of diffuser B was 0.070 of the diffuser-inlet total pressure, an increase of 0.027 from diffuser A (fig. 14).

Diffuser D produced a relatively uniform velocity profile (fig. 12(b)) and a pressure loss of 0.057 of the diffuser-inlet total pressure (fig. 14) as a result of removing the fourth and fifth downstream vanes of the five-vane cascade assembly of diffuser B.

Diffuser E, comprising the long inner cone and the second and third vanes from the cascade, produced a peak velocity of 600 feet per second (fig. 12(b)). The lowest local velocity, 140 feet per second, occurred on the center line of the burner. Total-pressure loss was 0.040 of the diffuser-inlet total pressure, the lowest value obtained for complete diffusion (fig. 14). Thus, low total-pressure loss and elimination of the reverse-flow area at the center were achieved in diffuser E. Average velocities for all diffusers were between 420 and 450 feet per second.

Diffuser F, which produced the velocity profile shown in figure 13, did not accomplish as complete a diffusion as the other diffusers, with the result that the average velocity was about 600 feet per second. Peak velocity was 780 feet per second at midpassage. Total-pressure loss was 0.038 of the diffuser-inlet total pressure (fig. 14).

Effect of velocity profile on performance. - The performance of the various configurations will be considered primarily in terms of afterburner combustion efficiency (see appendix for methods for calculation). The effect of the velocity profile or diffuser type on this parameter at the three diffuser-inlet total pressures is presented in figure 15. As given in table I, several configuration changes were made with the diffusers which appeared promising; but if the diffuser (with the exception of diffuser A) gave either a poor velocity profile or high pressure loss, less effort was used in optimizing the performance by flame-holder and fuel-system modifications. The futility of expending effort to improve performance with a poor velocity profile is shown in reference 1, where numerous fuel-system and flame-holder modifications were used with a relatively small improvement in performance. The best performance obtained with each diffuser type is presented herein.

As shown in figures 15(a) and (b), the variations in performance at pressure levels of 2750 and 1540 pounds per square foot were relatively small for the different velocity profiles at fuel-air ratios above 0.03. The larger variations below this fuel-air ratio are attributed to effects of fuel distribution. At the pressure level of 2750 pounds per square foot, the burner with diffuser E yielded the best performance, with a peak combustion efficiency of 0.99; while at the pressure level of 1540 pounds per square foot the highest combustion efficiency of 0.92 was obtained with diffuser B. As shown in figure 15(c), variations in

performance at the pressure level of 620 pounds per square foot were large. The peak combustion efficiency of 0.90 was obtained with the velocity profile provided by diffuser B. Performance of configurations with diffusers D, E, and F was adequate, while with diffuser A the combustion efficiency was very low. Peak combustion efficiency of the latter was 0.54 and represents the optimum as reported in reference 1.

Thus, good diffuser characteristics permitted an increase in combustion efficiency of about 0.30 above the best value obtainable with the original diffuser. With a poor velocity profile, as represented by diffuser A, it becomes necessary to burn the fuel in high-velocity regions; while with a more uniform distribution, as represented by diffusers B, D, and E, combustion takes place in more favorable environments. The data of figure 15 show that the effect of velocity profile on performance is particularly important at low afterburner-pressure levels.

Effect of fuel distribution on performance. - The effects of varying the radial fuel distribution on the combustion efficiency of configuration E1 are shown in figure 16. As explained under PROCEDURE, the radial distribution was altered by manipulation of three throttles, one of which controlled the flow to the inner three rings. A separate throttle was used for each of the outer two fuel-manifold rings. At a diffuser-inlet pressure level of 2750 pounds per square foot, three fuel distributions were used, as shown by the symbols and the key in figure 16(a). Although the peak efficiency for all three distributions was 0.99, the fuel-air ratio at which the peak efficiency occurred increased as the uniformity of the fuel distribution was improved. As noted in reference 2, this is to be expected, inasmuch as excessive local enrichment occurs with a stratified or nonuniform distribution at high over-all values of fuel-air ratio. Conversely, at low over-all fuel-air ratios, efficiencies are lower with the more uniform fuel distribution, because some local strata may be too lean to support combustion. The same effect was obtained at a diffuser-inlet pressure of 1540 pounds per square foot (fig. 16(b)); however, at this condition the peak efficiency was slightly higher (0.89 as compared with 0.84) for the less uniform fuel distribution.

At a diffuser-inlet pressure of 620 pounds per square foot (fig. 16(c)), the combustion is altered because of partial or complete blow-out of the flame-stabilizing elements. For example, the lower level of operation indicated by the broken curve is due to flame blow-out of a large portion of the flame holder. Although periscope observations were not made, previous observations have shown that the marked decrease in combustion efficiency with the more uniform fuel distribution at fuel-air ratios above 0.026 is probably the result of the progressive blow-out of the flame over a portion of one flame-holder element. Under the conditions at which partial blow-out may occur, the peak combustion efficiency occurred at a higher fuel-air ratio with the less uniform of the two fuel distributions. Thus, a fuel distribution which is selected as optimum at a low altitude may not be optimum at high altitudes.

The effect of changing radial fuel distribution in configurations using radial fuel-spray bars is shown in figure 17 for operation at a pressure level of 620 pounds per square foot. As was illustrated in figure 10, fuel system F was relatively uniform; whereas system G provided a rich mixture near the center of the afterburner, and system H provided a rich mixture near the flame-holder gutter. In this case, no partial flame blow-out was present, and the expected trends were obtained with the peak efficiency remaining about 0.73 for all three patterns and occurring at a higher fuel-air ratio with the most uniform distribution (F).

Previous investigations have indicated that operation with either 8 or 16 fuel-spray bars had little effect on afterburner performance; however, it is not certain how much the circumferential fuel distribution was altered because of the higher fuel pressure and consequent increased penetration of the fuel jets during operation with the smaller number of bars. Moreover, the effects on screeching combustion were unknown. Two sets of 10 fuel-spray bars, I and J (fig. 10), were constructed to provide a definite variation in the circumferential distribution and at the same time to maintain the same radial fuel distribution and fuel pressure. Observations of fuel-spray jets during afterburner operation through windows in the diffuser indicate the probable existence of a lean region immediately behind each spray bar and a relatively rich region a few inches on either side of the bar. In order to eliminate this lean region and to reduce the fuel in the rich regions, the dual side-spray holes of system J were replaced by single holes. Holes were then drilled at the same radial position to inject fuel in the upstream and downstream directions as well as sideways. These four-way spray bars comprised system I.

The effects of this change in circumferential fuel distribution on afterburner combustion efficiency are given in figure 18. As expected, the fuel-air ratio for peak combustion efficiency was higher with the four-way spray bars (I) because of the more uniform distribution. Also at the lowest pressure level of 620 pounds per square foot the peak efficiency was higher with the four-way spray bars. Thus it is shown that both circumferential and radial fuel distribution are important considerations in afterburner design.

Data with both systems in operation, providing 20 equally spaced bars, are also shown in figure 18 (configuration F9). Performance at the highest diffuser-inlet pressure, 2750 pounds per square foot, was somewhat poorer than that obtained with either I or J. At a diffuser-inlet pressure of 620 pounds per square foot, performance was intermediate between that obtained with the two sets of 10 bars. Although the circumferential fuel distribution was different with both systems in operation, no conclusions are possible because of the possible effects of the reduced fuel pressures occurring with both sets in operation.

In order to determine the effects of fuel pressure on afterburner performance and operational characteristics, two configurations, E1 and E2, were investigated. These configurations were identical, except that the fuel holes were 0.026 and 0.041 inch in diameter, respectively. Fuel pressures characteristic of the two configurations are given in figure 19. Fuel pressures for E1 were about 6 times as high as those for E2. The afterburner combustion efficiencies obtained are compared in figure 20. Although the performance was equal or better with the higher fuel pressures of configuration E1 at all three pressure levels, the expected trends did not occur. Although an improvement was expected at low fuel-air ratios during operation at a diffuser-inlet pressure of 620 pounds per square foot (because of elimination of "head" effects in the fuel rings), the improvement occurred at high fuel-air ratios. At the higher pressure levels where no effect was anticipated, the higher fuel pressure gave better performance. These improvements in performance are probably due to increased fuel penetration (and hence increased fuel droplet evaporation time) during operation with the higher fuel pressures. It should be noted, however, that the use of a total fuel-orifice area equal to that of E1 would result in fuel pressures greatly in excess of the pump-pressure limit at some flight conditions. Thus the need for a dual fuel system or a variable-area spray nozzle is indicated.

Effect of flame-holder type. - Previous experience has indicated that detailed flame-holder changes have relatively little effect on performance if the blockage is held constant and a reasonably suitable shape is used. Performance of flame holders C and D (fig. 9(c) and (d)) installed in configurations B1 and B2, respectively, is compared in figure 21 for operation at a diffuser-inlet pressure of 620 pounds per square foot. Although peak combustion efficiencies are both about 0.70 at a fuel-air ratio of 0.035, flame holder C provides higher efficiencies at fuel-air ratios above 0.035. Inasmuch as blockage for both flame holders was 40.5 percent, use of extra stabilizing bars between gutters probably accounts for the better performance of flame holder C.

Performance of best configuration. - The performance rating of the various configurations is ultimately based on two factors, thrust and specific fuel consumption. On the basis of these two factors, configuration E1, which comprised the long inner body and two vanes of the cascade assembly, gave slightly better performance than any other. As compared with configuration B3, the reduced diffuser pressure drop of configuration E1 more than compensated for the slightly lower combustion efficiencies obtained at some flight conditions. Values of augmented net thrust and specific fuel consumption of configuration E1 are presented in figure 22 for operation at different diffuser-inlet pressures.

Lower over-all specific fuel consumptions were obtained at the lowest pressure level of 620 pounds per square foot for operation at fuel-air ratios below 0.03, despite the fact that afterburner combustion efficiency was lower at 620 pounds per square foot than it was at higher pressures. This apparent discrepancy is explained by the fact that higher turbine-outlet temperatures were used at 620 pounds per square foot; thus a larger portion of the total fuel flow was consumed in the engine proper, where it was used more effectively than in an afterburner. This effect is, of course, largest at the lowest afterburner fuel-air ratios.

OPERATIONAL CHARACTERISTICS

The operable range of the configurations discussed herein was limited by several factors. The minimum operable afterburner fuel-air ratio was always limited by lean combustion blow-out, but the maximum operable fuel-air ratio was limited by the following factors: (1) maximum exhaust-nozzle area, (2) maximum afterburner fuel-pump pressure, (3) rich combustion blow-out, and (4) screeching combustion.

Screech in an afterburner is a type of combustion instability usually manifest by a marked change in the sound and often by a definite change in the flame color to an opaque white. There have, however, been some instances of screech not descernible to the ear. During this investigation, measurements with a panoramic sonic analyzer during screech showed the existence of large-amplitude pressure pulsations at frequencies between 800 and 6000 cycles per second. Other studies, however, show that screech may occur at frequencies between 400 and 10,000 cycles per second. Some examples of these pressure pulsations as a function of frequency (horizontal scale) are shown in figure 23. Although the vertical scale is indicative of the amplitude of the pressure pulsations, absolute values were not obtained because of a lack of data on the attenuation present in the instrumentation. Inasmuch as the point source of light swept the frequency range in 1 second and the film exposure time used was about 2 seconds, two and sometimes three traces appear, which indicate the time variation of the pressure pulses. Afterburner operation with and without screech is shown in figures 23(b) and 23(a), respectively. With screech, a pronounced peak occurs at a frequency of about 850 cycles per second. As shown in figure 23(c), however, large-amplitude pressure pulsations generally occur at several frequencies during screeching combustion. Irrespective of attenuation, the relative magnitudes of the pressure pulses shown in figure 23(d) for operation with and without screech are valid, inasmuch as no change in gain was made.

Experience at this laboratory and elsewhere (refs. 4 and 5) has shown that screeching combustion is extremely destructive, producing fatigue failure of welded seams or sometimes virgin metal in the afterburner shell generally 1 or 2 feet downstream of the flame holder. Welded seams may open, however, anywhere along the length of the combustion chamber. These failures may occur in a matter of seconds at

sea level, and in a few minutes at intermediate altitudes. At altitudes on the order of 45,000 feet, operation in screech has occurred for periods up to 5 minutes without damage. Data on screech are limited, and at present the causes are unknown.

The operable range of the configurations investigated herein and the factors limiting the operable range are given by the bar charts of figure 24, which indicate primarily normal operation, rich and lean combustion blow-out, screeching combustion, maximum fuel flow obtainable, and maximum exhaust-nozzle position. The characteristics of each configuration are discussed in the following paragraphs.

Configuration A1. - This configuration, made up of the original production diffuser (ref. 1), was one of the best configurations with respect to operation. This configuration was free of combustion instability, except for rumble which occurred with one fuel distribution at an afterburner fuel-air ratio of 0.041 at a diffuser-inlet total pressure of 1540 pounds per square foot (fig. 24(b)). The maximum fuel-air ratio was limited in all other instances by either the afterburner fuel-pump pressure or by the maximum area of the exhaust nozzle.

Configuration A2. - Configuration A2 differed from A1 in that a different fuel system and flame holder were used. The flame holder and fuel system were identical to those used in configuration E1. Configuration A2 was used only to check the effect of velocity profile on screeching characteristics. No screech occurred at any fuel flow up to the maximum obtainable at a diffuser-inlet total pressure of 2750 pounds per square foot.

Configuration B1. - Series B configurations operated with a flatter velocity profile than series A (fig. 12) because of the five-vane annular cascade assembly. Screeching combustion did not occur with configuration B1, although burning on the outer gutter of the flame holder was erratic and propagation between gutters appeared poor at a diffuser-inlet total pressure of 620 pounds per square foot.

Configuration B2. - In an attempt to improve flame propagation between gutters, flame holder C was replaced with flame holder D (fig. 9), forming configuration B2. This configuration did not screech, but visual observation showed no improvement in flame propagation between the gutters.

Configuration B3. - Configuration B3 was formed from B2 by replacing the 3-V-gutter flame holder with a staggered 2-V-gutter flame holder (fig. 9(b)) and by turning the five-ring fuel manifold around to spray upstream. No screech occurred at any diffuser-inlet total-pressure level investigated. The afterburner would ignite and operate at a diffuser-inlet total pressure of 620 pounds per square foot.

Configuration C1. - In an effort to reduce the diffuser pressure losses associated with the five-ring annular cascade, a long diffuser inner cone incorporating vortex generators on its upstream end was installed, forming configuration C1 (fig. 4(c)). As shown in figure 12, the velocity profile was poor. Although no screech was encountered at any diffuser-inlet total-pressure level at or below 2750 pounds per square foot, stable burning could not be obtained at 620 pounds per square foot.

Configuration D1. - Configuration D1 was identical to B3, except that the last two vanes were removed from the annular cascade to reduce the pressure loss. The operational characteristics were almost the same as B3 down to a pressure level of 620 pounds per square foot.

Configuration E1. - The series E configurations incorporated a long diffuser inner cone and the second and third vanes from the annular cascade assembly (fig. 4(c)). The velocity profile was not quite as uniform as those obtained with series B and D configurations. The operational characteristics of configuration E1 were good at all diffuser-inlet total pressures investigated down to and including 620 pounds per square foot. A check revealed that the afterburner would not ignite at a diffuser-inlet total pressure of 490 pounds per square foot.

Configuration E2. - Because the total fuel-orifice area used with configuration E1 would result in excessive fuel pressures at low-altitude - high-speed flight conditions, the fuel-orifice size was increased from 0.026- to 0.041-inch diameter to form configuration E2. Operational characteristics were almost identical to those of configuration E1.

Configuration E3. - Configuration E3 was identical to E1 and E2, except for a change in the fuel system. The three-ring fuel manifold used in configuration E3 sprayed the fuel in a radial direction instead of axially (fig. 10(d)). Ignition was easily obtained and burning was steady at the minimum diffuser-inlet total pressure obtainable of approximately 411 pounds per square foot. The tendency for screech was checked at diffuser-inlet total pressures up to 3270 pounds per square foot (maximum obtainable); however, no screech was encountered, with one brief exception at a diffuser-inlet total pressure of 2750 pounds per square foot. Screech at this condition could not be repeated. At very high pressures, the inner flame-holder gutter did not hold flame, perhaps as a result of change in fuel penetration in the radial direction. Also at high diffuser-inlet total pressures, 2750 and 1540 pounds per square foot, the lean blow-out limit was almost the same as E2; however, at 620 pounds per square foot, the lean limit of configuration E3 was much lower.

Configuration E4. - Configuration E4 was the same as E3, except that the fuel-orifice sizes were increased and additional holes were drilled in the rings to reduce the fuel pressure. The resulting low fuel pressure apparently produced a "head" effect in the fuel manifold, resulting in a void or nonburning region at the top of the burner when operating at a diffuser-inlet total pressure of 620 pounds per square foot. Also at this pressure level, rich combustion blow-out occurred at rather low values of fuel-air ratio, 0.060 to 0.068.

Configuration F1. - The series F configurations, incorporating a large diffuser inner cone and single-V-gutter flame holder (fig. 8), did not provide a uniform velocity pattern at the plane of the flame holder (fig. 13). As shown in figure 24(b), the operable range of configuration F1 at a diffuser-inlet total pressure of 1540 pounds per square foot was extremely narrow. Lean blow-out occurred at a fuel-air ratio of 0.030, and the exhaust nozzle was driven wide open at about 0.0355 fuel-air ratio. Screech occurred intermittently at a fuel-air ratio of 0.0335 for operation using 10 of the 20 spray bars. With 20 spray bars, the screech was much louder and occurred over the entire operable range. This reduced tolerance to screech, exhibited when 20 fuel-spray bars were used, was also demonstrated at diffuser-inlet total pressures of 620 and 2750 pounds per square foot. At a pressure level of 620 pounds per square foot, screech was encountered with 20 spray bars at a fuel-air ratio of 0.06; with 10 spray bars, the exhaust nozzle was driven open at a fuel-air ratio of 0.055.

Configuration F2. - Configuration F2 was the same as F1, except that the fuel pattern, using 10 fuel bars, concentrated the fuel much nearer the diffuser inner body (fig. 10). As shown in figure 24(a) and (b), screech occurred at both 2750 and 1540 pounds per square foot diffuser-inlet total pressure. The fuel-air ratio at the latter condition was about the same as configuration F1 operating with 10 fuel-spray bars. At a diffuser-inlet total pressure of 620 pounds per square foot, no screech occurred. Rich combustion blow-out occurred at a high fuel-air ratio, 0.105; and lean blow-out occurred at 0.034, a value somewhat lower than that for configuration F1.

Configuration F3. - The 10 fuel bars of configuration F3 concentrated the fuel in line with the flame-holder gutter rather than near the inner body as in configuration F2. Otherwise F3 was identical to F1 and F2. The screech limits were about the same as F2, except at a diffuser-inlet total pressure of 620 pounds per square foot where screech occurred at a fuel-air ratio of 0.054. Also at this pressure level, the lean blow-out limit was considerably lower than that of F2. Operating the combined fuel systems of F2 and F3 had no appreciable effect on the screech limit at 2750 pounds per square foot diffuser-inlet total pressure.

Configuration F4. - Configurations F4, F5, and F6 were identical to F1, F2, and F3, except for the spray bars. The radial fuel pattern of configuration F3 was retained (rich near the flame-holder gutter); however, changes were made to alter the fuel penetration and hence the circumferential fuel distribution. For configuration F4, the fuel bars of F3 were altered by drilling holes at the same radial location, perpendicular to the original holes, to provide a fuel spray in the upstream and downstream directions as well as circumferentially (fig. 10). This change, which reduced the circumferential penetration, had little effect on screech except at a diffuser-inlet total pressure of 620 pounds per square foot, where screech occurred at a slightly lower fuel-air ratio. Lean blow-out limits did not change appreciably.

Configuration F5. - To form configuration F5, the holes in fuel bar H used with configuration F3 were duplicated 1/8 inch radially inward (fig. 10), thus retaining essentially the same radial fuel-air distribution while reducing the penetration. Also, the fuel concentration immediately downstream of a fuel bar should be less than for configuration F4. Both the screech and the lean blow-out limits for F5 and F4 were almost identical. At a diffuser-inlet total pressure of 620 pounds per square foot, the screech limit was slightly above the value required to drive the exhaust nozzle open. Hence, this limit occurred with the engine operating slightly above limiting turbine-outlet temperature.

Operational procedure was found to have an important effect on the screech limits. This phenomenon may be illustrated by referring to figure 24(b). At a diffuser-inlet total pressure of 1540 pounds per square foot, screech was encountered as the fuel-air ratio was being increased at a value of 0.0297 (upper half of bar). To determine the possible existence of a screech-free region at higher fuel-air ratios, the throttle was "jammed" open quickly to a fuel-air ratio of about 0.047; but the screech persisted, and the afterburner was shut off. The afterburner was then reignited (lower half of bar) at a high fuel-air-ratio point (a); but no screech occurred, even though the fuel-air ratio was gradually decreased throughout the previous screech range to point (b). When the fuel-air ratio was again increased, screech occurred (point (c)) at almost exactly the same fuel-air ratio as that previously determined. Thus, it is evident that the direction of approach to the screech fuel flow has a marked bearing on screech limits.

Configuration F6. - Configuration F6 used the fuel-spray bars of F4 and F5 simultaneously. Lean blow-out limits were not affected by the combination; however, the screech limit was shifted to a higher fuel-air ratio at a diffuser-inlet total pressure of 1540 pounds per square foot. At a pressure level of 620 pounds per square foot, screech was not encountered with configuration F6.

Configurations F7, F8, and F9. - Configurations F7, F8, and F9 were identical to F4, F5, and F6, except that 1/4-inch-high flat strips were attached to the trailing edges of all flame-seat surfaces. At a diffuser-inlet total pressure of 2750 pounds per square foot, the addition of the strips did not appear to affect the lean blow-out limit; but screech occurred at slightly higher fuel-air ratios. At a diffuser-inlet total pressure of 1540 pounds per square foot, a comparison of configuration F4 and F7 and F5 with F8 shows that the addition of strips markedly reduced the screech range. At a diffuser-inlet total pressure of 620 pounds per square foot, no screech occurred within the operating range. It should be noted, however, that the maximum fuel-air ratio was limited by the opening of the exhaust nozzle to values below those which produced screech in the configurations without the strips. In general, it appears that the addition of the strips had a beneficial effect in reducing the tendency for screech.

Inspection of the bar charts of figure 24 shows that the configurations employing diffuser F, which provided high velocities near the flame holder, were much more prone to screeching combustion than were the other configurations. Also, it was shown that changes in either radial or circumferential distribution or the addition of flat strips to the trailing edges of the flame-holder gutter had little effect on screech in these configurations. Although the available information does not warrant a definite conclusion, it appears that high velocities at the flame-holder gutters may increase the tendency to screech.

The effect of diffuser-inlet total pressure and fuel-air ratio on lean blow-out and screech limits is shown in figure 25 for 15 configurations. For most configurations the fuel-air ratio for lean blow-out increased slightly as the diffuser-inlet total pressure was reduced. In all cases, the fuel-air ratio at which screech occurred increased as the pressure was reduced. Typical limit curves are shown (fig. 25), and it will be noted that the operable range between these two limits increased as the pressure was reduced. The operating region defined in this figure shows the general regions of stability and is believed to be indicative of the general trends of screech and blow-out limits.

The effect of fuel type on screech limits was checked with configuration F7 with MIL-F-5624A (grades JP-3 and JP-4) fuels at a diffuser-inlet total pressure of 1540 pounds per square foot. Screech occurred at the same fuel-air ratio with both fuels as the fuel was increased, but the rich screech limit occurring as fuel flow was decreased from a high value occurred at a fuel-air ratio of 0.039 with grade JP-3 as compared with 0.035 with JP-4 fuel. At a diffuser-inlet total pressure of 2750 pounds per square foot, it was impossible to operate above the lean screech limit, which was identical for both grades of fuel.

Because the work of reference 5 showed that detonation might be responsible for a certain type of combustion instability, tetraethyl lead was added to the grade JP-3 fuel. The use of this detonation suppression had no effect on the screech limit.

A brief attempt was made to determine the effect of burner-inlet temperature on screech by holding the afterburner fuel-air ratio constant and varying the diffuser-inlet temperature by adjusting the position of the variable-area exhaust nozzle. The data, obtained with configuration E4 (fig. 26), show that the screech limit of this configuration is not affected appreciably by the burner-inlet temperature in the range from 965° to 1110° F.

CONCLUDING REMARKS

Several afterburner configurations including six diffuser designs and numerous modifications to the fuel system and flame holders were studied, with the diffuser design as the primary variable. At the lowest diffuser-inlet total pressure used, 620 pounds per square foot, the velocity profile provided by the diffuser at the burner inlet had a large effect on the afterburner combustion efficiency. At this pressure level, peak combustion efficiency of only 0.54 was obtained with a velocity profile which varied from 630 feet per second near the outer flame-holder gutter to zero velocity or reverse flow near the center line of the burner. In contrast, a peak efficiency of 0.90 was possible with a velocity profile which varied from a maximum value of 590 feet per second near the shell to a velocity of about 430 feet per second at the center line. The latter profile, however, provided a velocity as low as 220 feet per second near the flame-holder gutters.

At a pressure level of 2750 pounds per square foot, the peak combustion efficiency was 0.99 for the three radial fuel distributions used; however, the fuel-air ratio at which the peak occurred increased when the most uniform fuel-air pattern was used. This trend, which was to be expected, did not occur at the lowest pressure level of 620 pounds per square foot, because of partial blow-out of the flame-stabilizing elements. Hence, a fuel distribution selected as optimum at low altitudes may not be optimum at high altitudes. It was also found that an increase in fuel-orifice size to permit operation without excessive fuel-pump pressures at low altitudes impaired the performance at high altitudes.

Screeching combustion, which was most prevalent at low altitudes and medium-to-high fuel-air ratios, imposed a restriction on the operable range of a number of configurations. The configurations incorporating a diffuser which produced very high velocity near the flame-holder gutters were much more prone to screech. The addition of

flat strips to the flame-holder trailing edges and variations in either the radial or circumferential fuel distribution had no large effect on the screech limits. Neither the addition of tetraethyl lead to the fuel nor a reduction in burner-inlet temperature from 1110° to 965° F had any appreciable effect on screeching combustion or the fuel-air ratio at which it occurred.

Lewis Flight Propulsion Laboratory
National Advisory Committee for Aeronautics
Cleveland, Ohio, January 7, 1953

APPENDIX - CALCULATIONS

Symbols

The following symbols are used in this report:

A	cross-sectional area, sq ft
B	thrust-scale reading, lb
C_v	velocity coefficient, ratio of scale jet thrust to rake jet thrust
D	external drag of installation, lb
D_r	drag of exhaust-nozzle survey rake, lb
F_j	jet thrust, lb
F_n	net thrust, lb
f/a	fuel-air ratio
g	acceleration due to gravity, 32.2 ft/sec^2
H	total enthalpy of air, Btu/lb
P	total pressure, lb/sq ft abs
p	static pressure, lb/sq ft abs
R	gas constant, 53.4 ft-lb/(lb)($^\circ$R)
T	total temperature, $^\circ$R
t	static temperature, $^\circ$R
V	velocity, ft/sec
W_a	air flow, lb/sec
W_f	fuel flow, lb/hr
W_g	gas flow, lb/sec
$\frac{W_{f,t}}{F_{n,s}}$	specific fuel consumption based on total fuel flow and scale net thrust, lb/(hr)(lb thrust)

γ ratio of specific heats for gases

η combustion efficiency

λ total enthalpy of fuel, Btu/lb

Subscripts:

a air

b afterburner

e engine

f fuel

i indicated

j jet

s scale

t total

x inlet duct at frictionless slip joint

0 free-stream conditions

1 engine-inlet duct

5 turbine inlet

5' first-stage turbine-nozzle throat

6 diffuser inlet (turbine outlet)

7 diffuser outlet (burner inlet)

9 exhaust nozzle

Methods of Calculation

Temperatures. - Static temperatures were determined from thermocouple-indicated temperatures with the following relation:

$$t = \frac{T_i}{1 + 0.85\left[\left(\frac{P}{p}\right)^{\frac{\gamma-1}{\gamma}} - 1\right]} \tag{1}$$

where 0.85 is the impact recovery factor for the type thermocouple used. Total temperatures were determined by the adiabatic relation between temperatures and pressures.

Airspeed. - The equivalent airspeed was calculated from ram-pressure ratio by the following equation, with complete pressure recovery at the engine inlet assumed:

$$V_0 = \sqrt{\frac{2\gamma_1 g R T_1}{\gamma_1 - 1}\left[1 - \left(\frac{p_0}{P_1}\right)^{\frac{\gamma_1-1}{\gamma_1}}\right]} \tag{2}$$

Air flow and gas flow. - Because of erratic measurements at the engine inlet during the afterburning program, the air flow was determined from measurements at the turbine inlet (station 5). Since the turbine nozzles were choked for the range of conditions investigated, the gas flow at the turbine nozzle throat could be determined from the following equation:

$$W_{g,5'} = \frac{P_5 A_{5'}}{\sqrt{T_5}}\sqrt{\frac{g}{R}}\,\frac{\sqrt{\gamma_5}}{\left(\frac{\gamma_5+1}{2}\right)^{\frac{\gamma_5+1}{2(\gamma_5-1)}}} \tag{3}$$

The effective turbine-nozzle throat area $A_{5'}$ was determined from previous tests for the same range of engine operating conditions investigated herein when the engine-inlet air-flow calculations were reliable. The air flow or gas flow at any station throughout the engine and afterburner could then be obtained from $W_{g,5'}$ by adding or subtracting the various factors of engine fuel flow, afterburner fuel flow, and compressor bleed air.

Afterburner fuel-air ratio. - The afterburner fuel-air artio is defined as the ratio of the weight flow of fuel injected in the afterburner to the weight flow of unburned air entering the afterburner

from the engine. Weight flow of unburned air was determined by assuming that the fuel injected in the engine was completely burned. This assumption of 100-percent combustion efficiency in the engine results in only a small error in afterburner fuel-air ratio, because the engine was operated where η_e is known to be high. Afterburner fuel-air ratio was calculated from the equation

$$(f/a)_b = \frac{W_{f,b}}{3600\, W_{a,6} - \frac{W_{f,e}}{0.067}} \tag{4}$$

where 0.067 is the stoichiometric fuel-air ratio for the engine fuel.

Exhaust-gas total temperature. - The total temperature of the exhaust gas was calculated from the exhaust-nozzle-outlet total pressure, scale jet thrust, velocity coefficient, and gas flow by means of the following equation:

$$T_j = \left(\frac{F_{j,s}}{C_v}\right)^2 \frac{g}{2R} \frac{\gamma_9 - 1}{\gamma_9} \frac{1}{W_{g,9}^2 \left[1 - \left(\frac{p_0}{p_9}\right)^{\frac{\gamma_9 - 1}{\gamma_9}}\right]} \tag{5}$$

The velocity coefficient C_v, which is defined as the ratio of scale jet thrust to rake jet thrust, was determined to be 0.98 from nonafterburning data over a wide range of exhaust-nozzle pressure ratios.

Combustion efficiency. - Afterburner combustion efficiency was obtained by dividing the enthalpy rise through the afterburner by the heat content of the afterburner fuel and unburned engine fuel as shown in the following equation:

$$\eta_b = \frac{3600\, W_{a,6} (H_{a,9} - H_{a,6}) + W_{f,e} (\lambda_{e,9} - \lambda_{e,6}) + W_{f,b} \lambda_{b,9}}{18{,}700\, W_{f,b} + (1 - \eta_e)\, W_{f,e}\, 18{,}700} \tag{6}$$

where 18,700 (Btu/lb) is the lower heating value of the engine fuel and afterburner fuel. The enthalpies of the products of combustion were determined from temperature-enthalpy charts for air and from temperature-enthalpy charts for fuels having the same hydrogen-carbon ratios as the fuels used in this investigation (see ref. 6). The charts used for obtaining fuel enthalpies were based on a fuel-inlet temperature of 80° F. Dissociation was not considered in this analysis, because its effect is negligible for the range of exhaust-gas temperatures encountered in this investigation.

Augmented thrust. - The jet thrust of the installation was determined from the balance-scale measurements by the following equation:

$$F_{j,s} = B + D + D_r + \frac{W_{a,1}V_x}{g} + A_x (p_x - p_0) \qquad (7)$$

The last two terms of this expression represent momentum and pressure forces on the installation. External drag of the installation was determined with the engine inoperative, and the drag of the water-cooled exhaust-nozzle survey rake was measured by an air-balance piston mechanism.

Scale net thrust was obtained by subtracting the equivalent free-stream momentum of the inlet air from the scale jet thrust:

$$F_{n,s} = F_{j,s} - W_{a,1}V_0/g \qquad (8)$$

REFERENCES

1. Conrad, E. William, and Campbell, Carl E.: Altitude Investigation of Several Afterburner Configurations for the J40-WE-8 Turbojet Engine. NACA RM E52L10, 1953.

2. Conrad, E. William, and Campbell, Carl E.: Altitude Wind Tunnel Investigation of High-Temperature Afterburners. NACA RM E51L07, 1952.

3. Wood, Charles C.: Preliminary Investigation of the Effects of Rectangular Vortex Generators on the Performance of a Short 1.9:1 Straight-Wall Annular Diffuser. NACA RM L51G09, 1951.

4. Fenn, J. B., Forney, H. B., and Garman, R. C.: Burners for Supersonic Ramjets. Bumblebee Rep. No. 119, Experiment Inc., Jan. 1950. (Contract NOrd 9756, Bur. Ordnance, U. S. Navy.)

5. Bragdon, Thomas A., Lewis, George D., and King, Charles H.: Interim Report on Experimental Investigation of High Frequency Oscillations in Ram-Jet Combustion Chambers. M.I.T Meteor Rep. UAC-53, Res. Dept,. United Aircraft Corp., Oct. 1951. (BuOrd Contract NOrd 9845.)

6. Turner, L. Richard, and Bogart, Donald: Constant-Pressure Combustion Charts Including Effects of Diluent Addition. NACA Rep. 937, 1949. (Supersedes NACA TN's 1086 and 1655.)

TABLE I. - SUMMARY OF CONFIGURATION DETAILS

Diffuser	Configuration	Flame holder			Fuel system			
		Designation	Location of leading edge, in. downstream of diffuser inlet	Blockage, percent	Designation	Location, in. downstream of diffuser inlet	Number of rings or bars	Direction of injection
A	1	A	$42\frac{5}{16}$	41.3	A	Inner 2- $41\frac{13}{16}$ Outer- $33\frac{9}{16}$	3 rings	Varied
	2	B	$38\frac{9}{16}$	33.9	B	$27\frac{7}{8}$	5 rings	Upstream
B	1	C	$38\frac{9}{16}$	40.6	B	$22\frac{3}{8}$	5 rings	Downstream
	2	D	$38\frac{9}{16}$	40.5	B	$22\frac{3}{8}$	5 rings	Downstream
	3	B	$38\frac{9}{16}$	33.9	B	$22\frac{3}{8}$	5 rings	Upstream
C	1	A	$42\frac{5}{16}$	41.3	C	$41\frac{13}{16}$	5 rings	Downstream
D	1	B	$38\frac{9}{16}$	33.9	B	$22\frac{7}{8}$	5 rings	Upstream
E	1	B	$38\frac{9}{16}$	33.9	B	$27\frac{7}{8}$	5 rings	Upstream
	2	B	$38\frac{9}{16}$	33.9	C	$27\frac{7}{8}$	5 rings	Upstream
	3	B	$38\frac{9}{16}$	33.9	D	$27\frac{7}{8}$	3 rings	Varied
	4	B	$38\frac{9}{16}$	33.9	E	$27\frac{7}{8}$	3 rings	Varied
F	1	E	$21\frac{5}{8}$	21.4	F	6	20 bars	Side
	2	E	$21\frac{5}{8}$	21.4	G	6	10 bars	Side
	3	E	$21\frac{5}{8}$	21.4	H	6	10 bars	Side
	4	E	$21\frac{5}{8}$	21.4	I	6	10 bars	4-way
	5	E	$21\frac{5}{8}$	21.4	J	6	10 bars	Side
	6	E	$21\frac{5}{8}$	21.4	I and J	6	20 bars	Varied
	7	F	$21\frac{5}{8}$	25.6	I	6	10 bars	4-way
	8	F	$21\frac{5}{8}$	25.6	J	6	10 bars	Side
	9	F	$21\frac{5}{8}$	25.6	I and J	6	20 bars	Varied

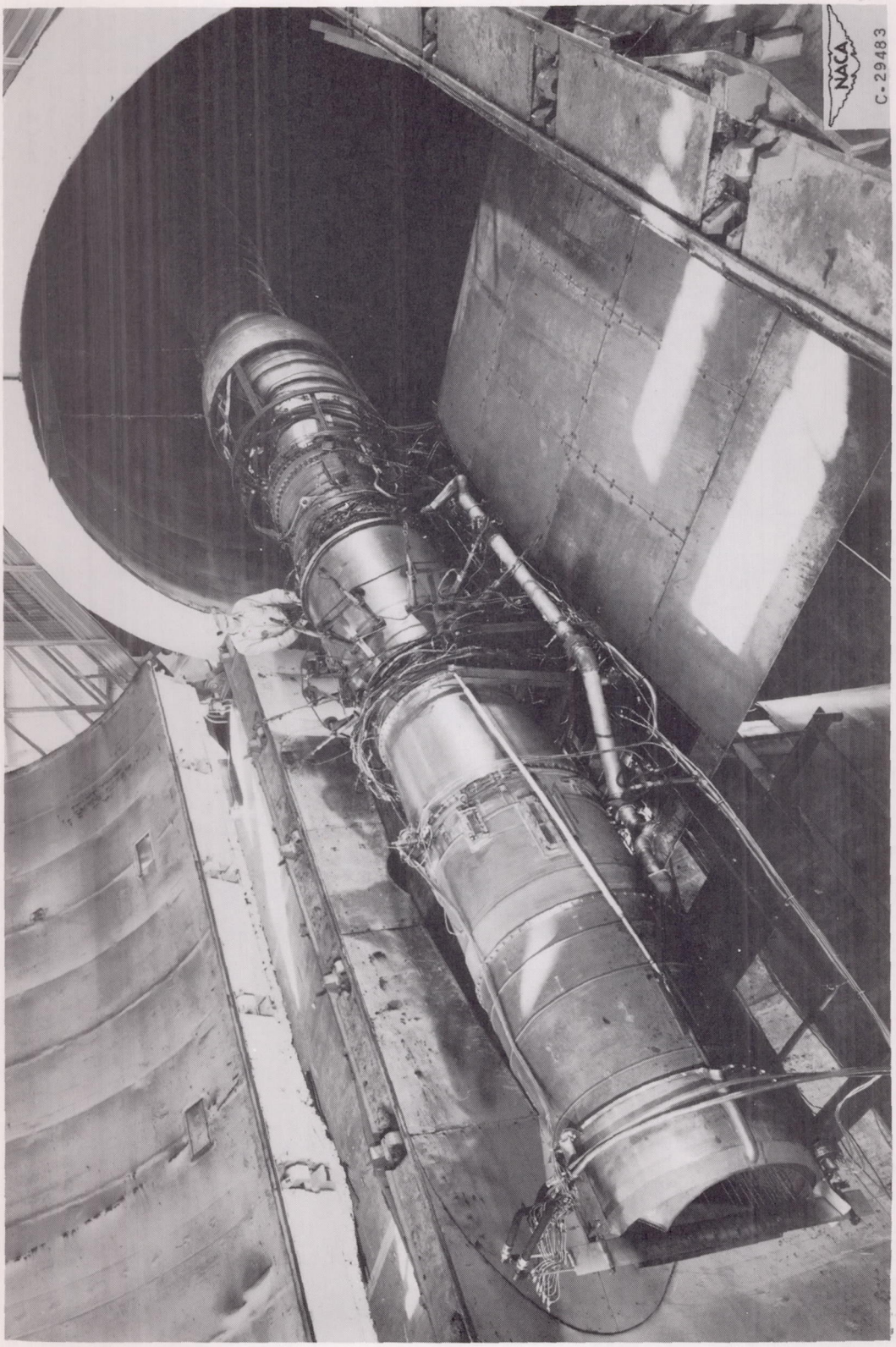

Figure 1. - View of engine installed in altitude wind tunnel.

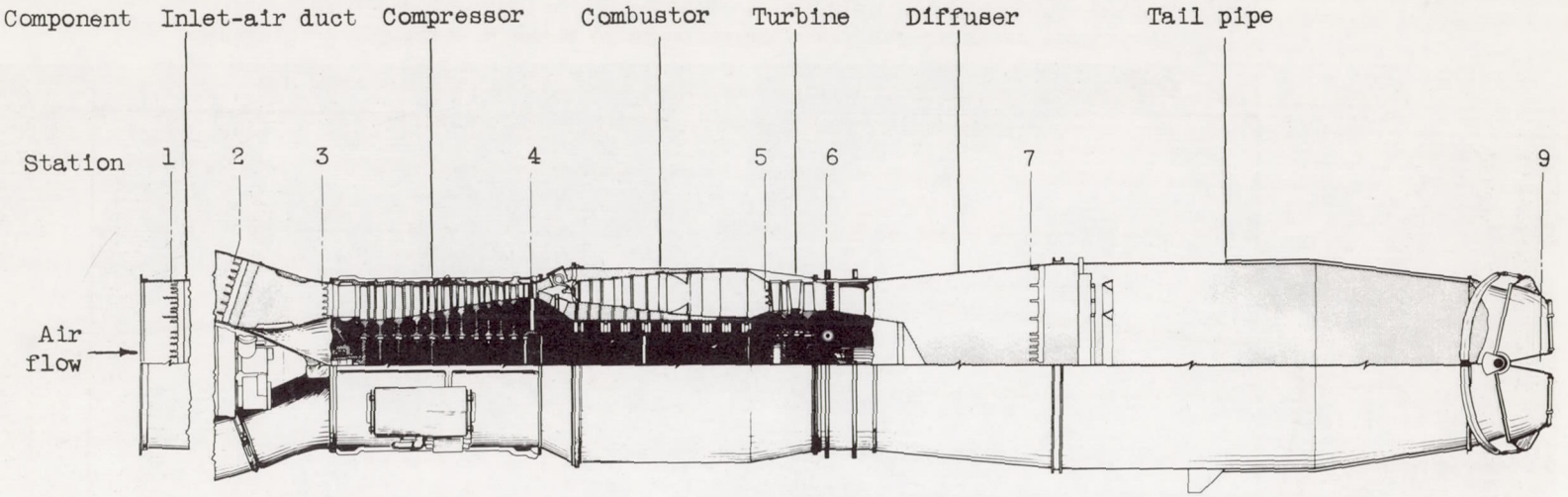

Station	Location	Total-pressure tubes	Static-pressure tubes	Wall static-pressure orifices	Thermo-couples
1	Inlet-air duct	29	12	6	10
2	Engine inlet	18	0	4	0
3	Compressor inlet	23	3	7	0
4	Compressor outlet	18	0	3	6
5	Turbine inlet	5	0	0	[a]10
6	Turbine outlet	20	0	8	24
7	Diffuser outlet	21	0	2	0
[b]7	Diffuser outlet	8	0	2	0
9	Exhaust-nozzle outlet	17	6	0	0

[a]Sonic probes
[b]Used for configuration F

NACA
CD-2860

Figure 2. - Cross section of engine showing stations at which instrumentation was installed.

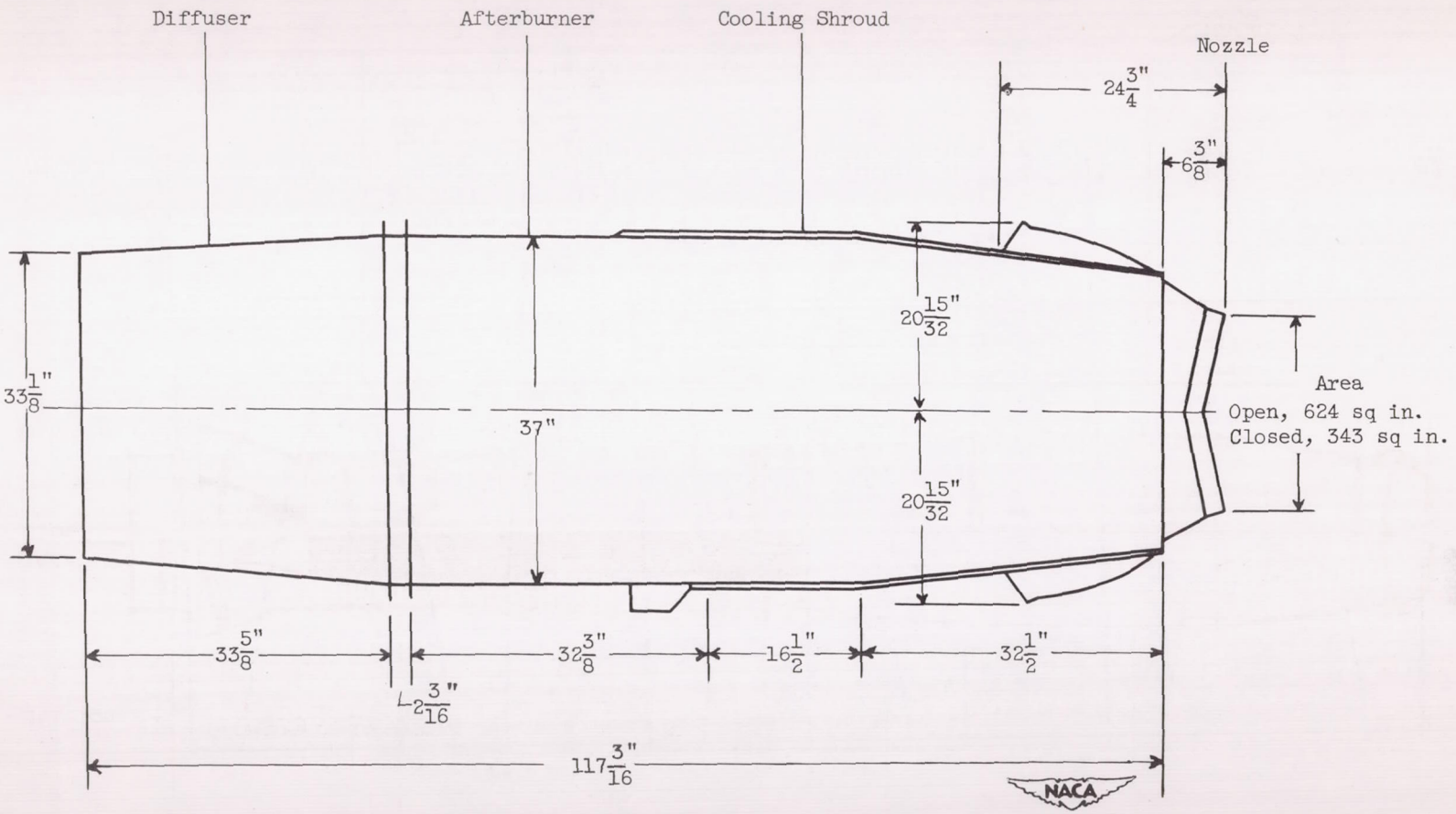

Figure 3. - Schematic drawing of afterburner shell and diffuser section.

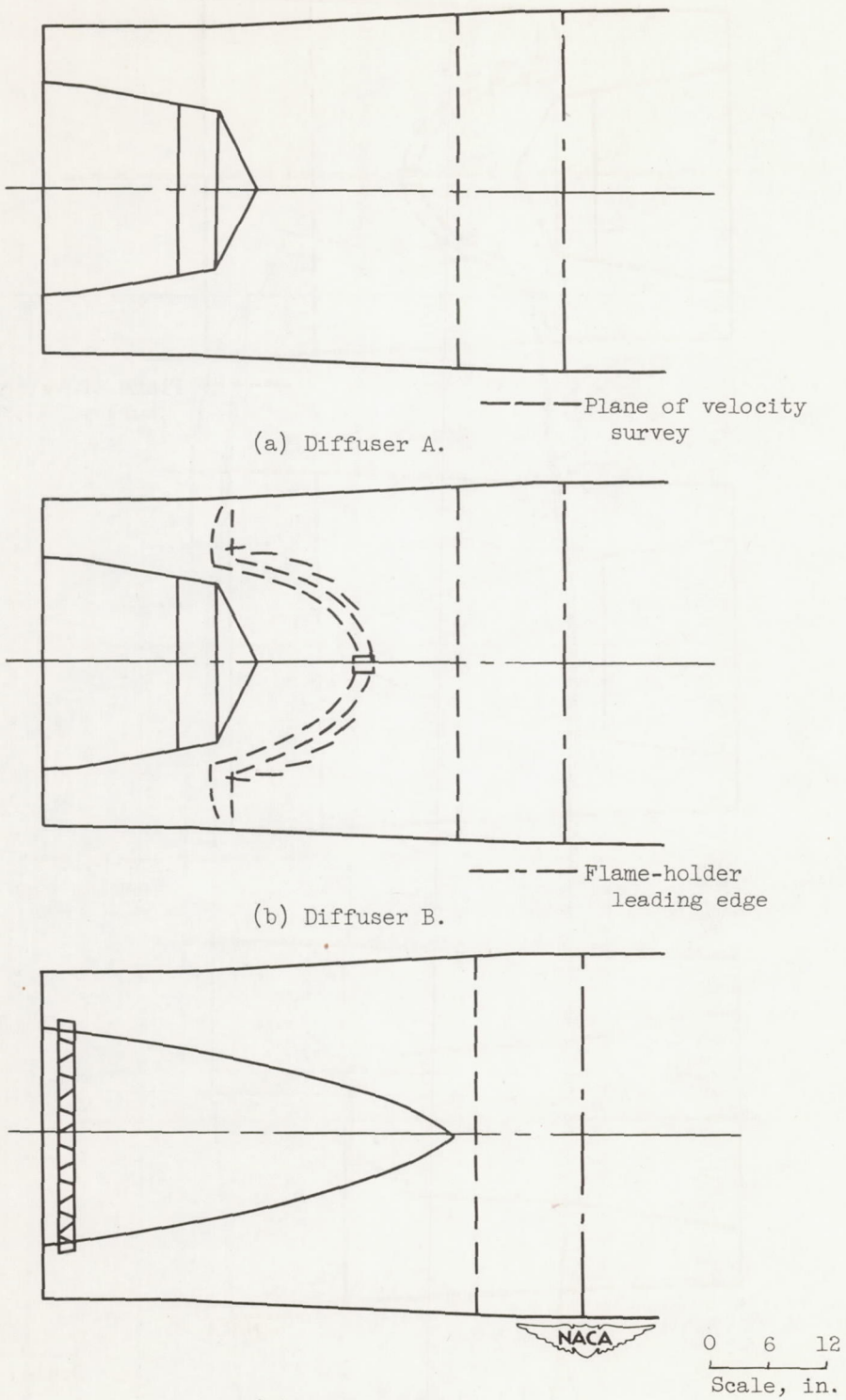

(a) Diffuser A.

(b) Diffuser B.

(c) Diffuser C.

Figure 4. - Diffuser types investigated.

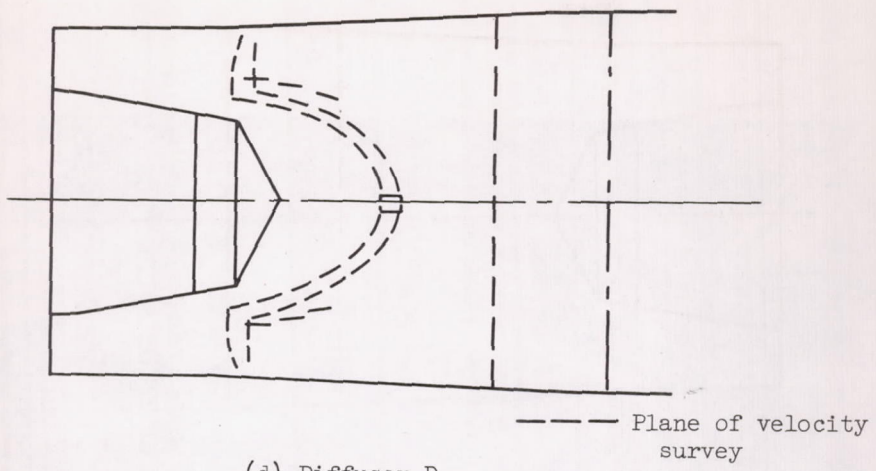

(d) Diffuser D.

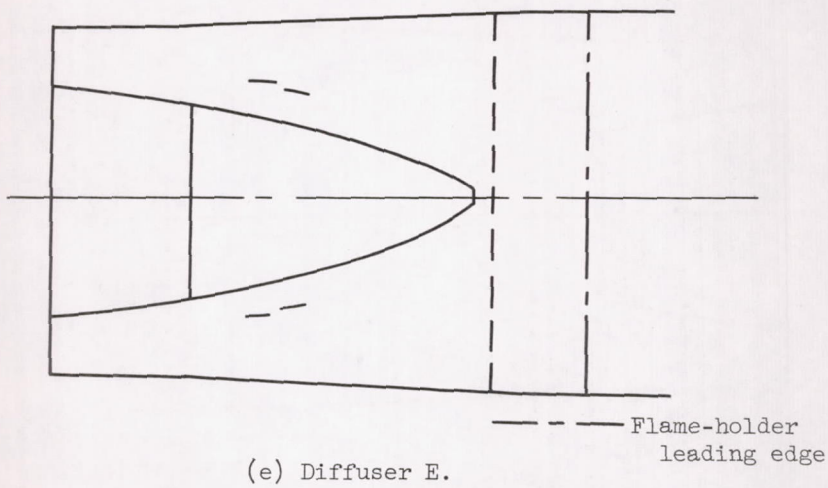

(e) Diffuser E.

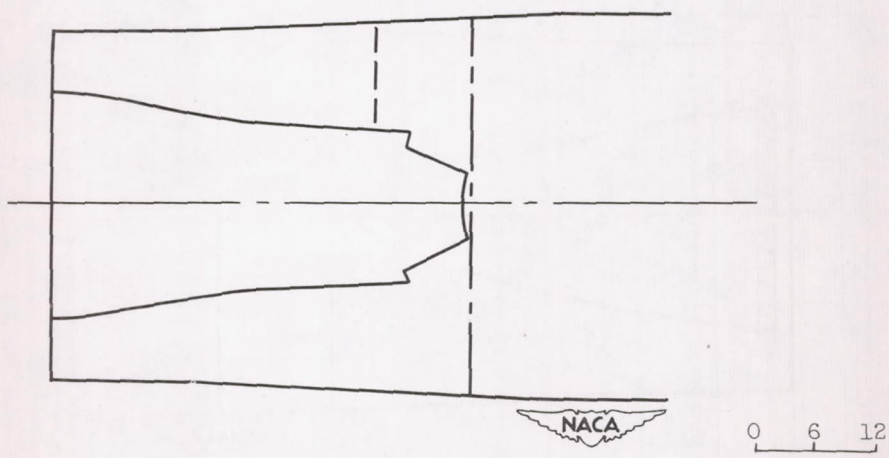

(f) Diffuser F.

Figure 4. - Concluded. Diffuser types investigated.

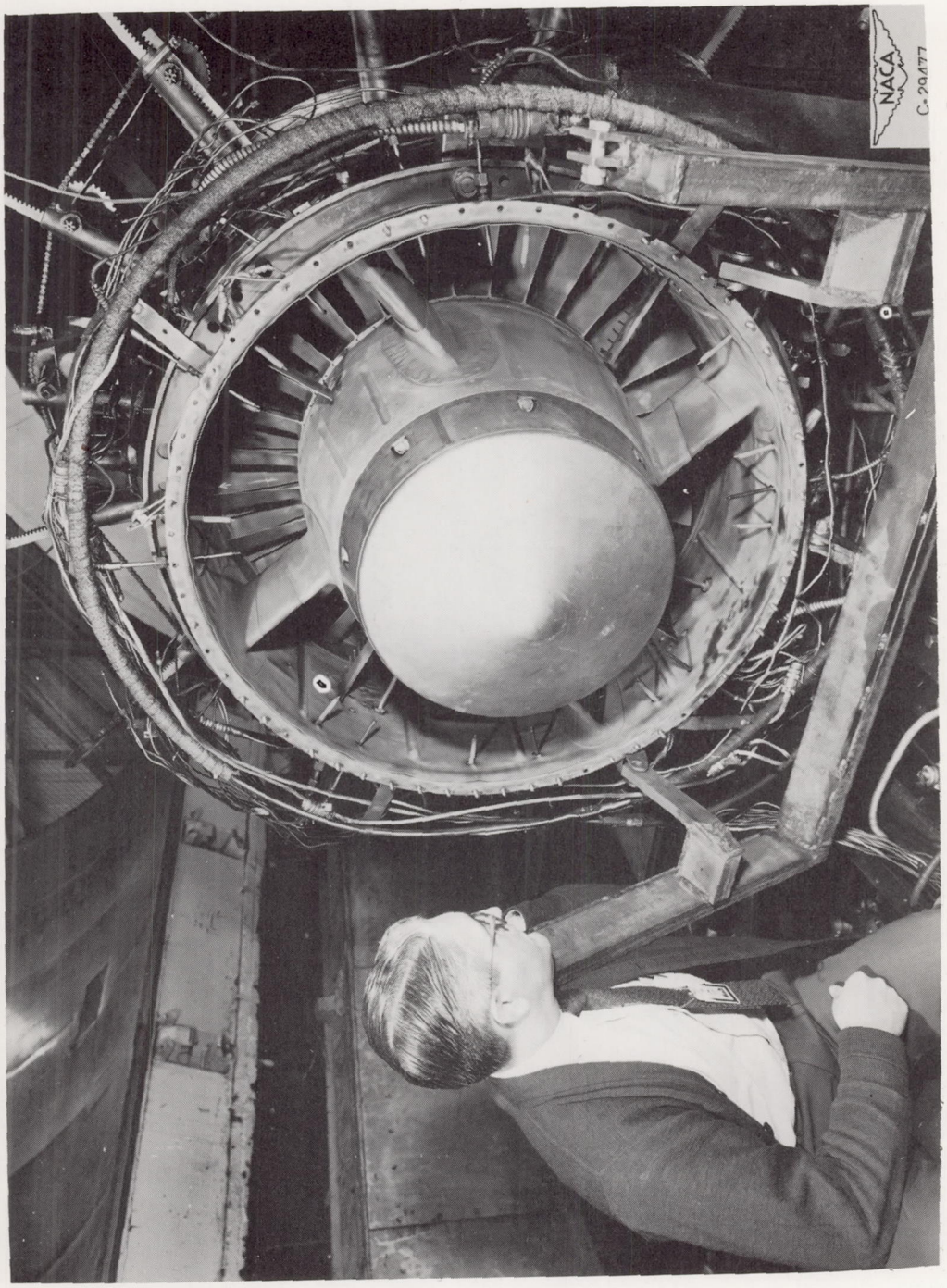

Figure 5. - View of diffuser A.

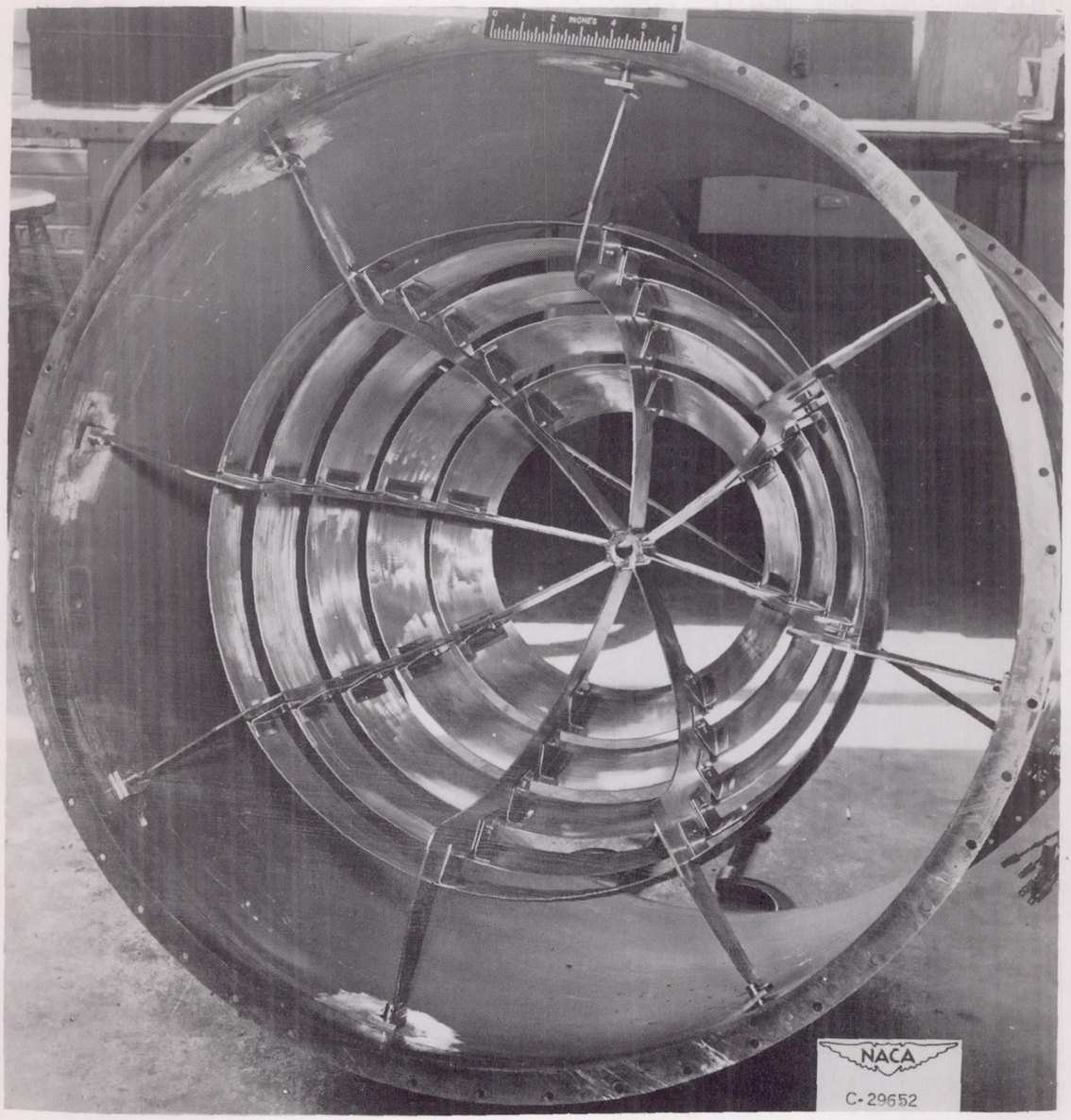

Figure 6. - View of annular cascade assembly used in diffuser B.

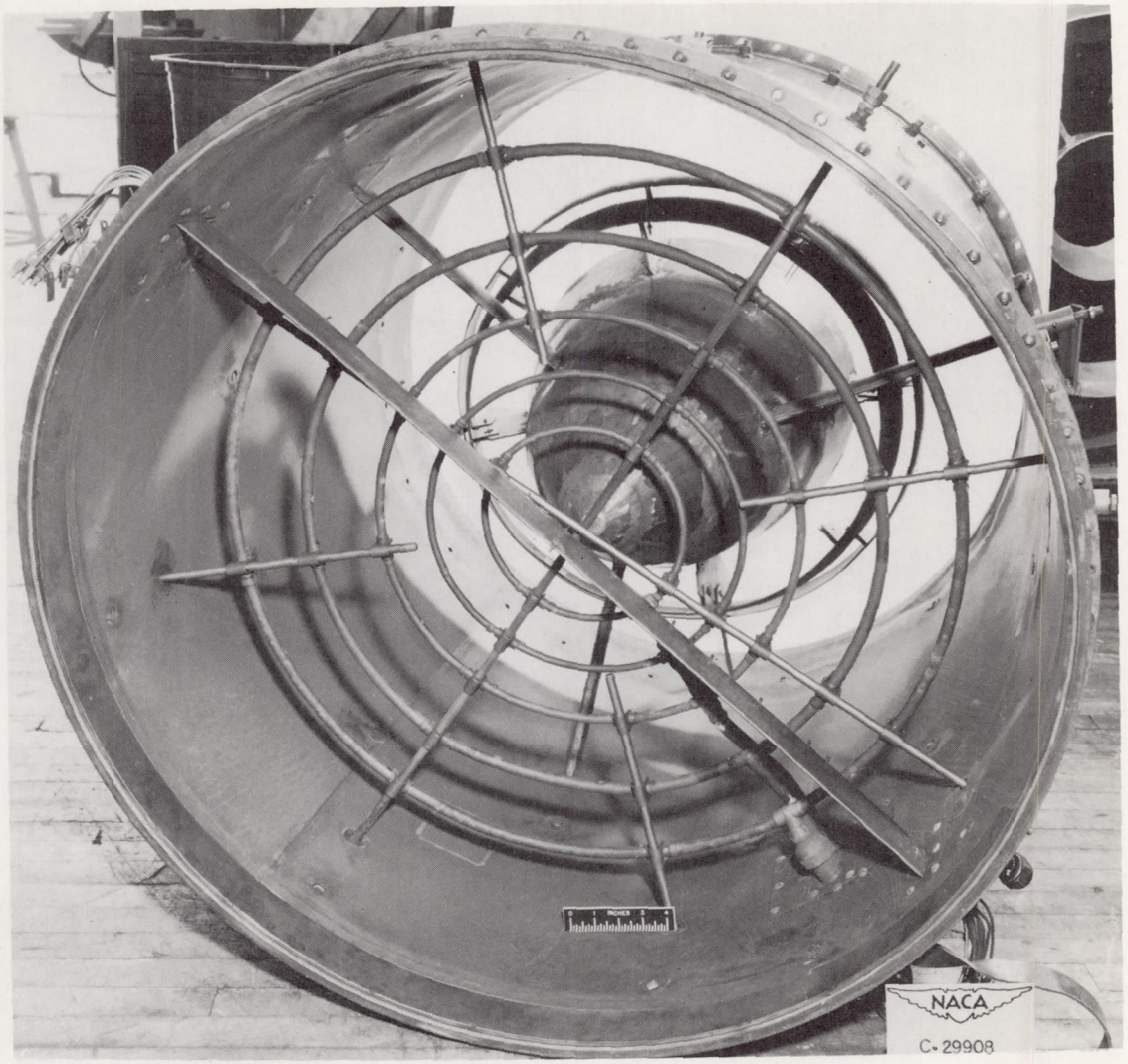

Figure 7. - View of diffuser E.

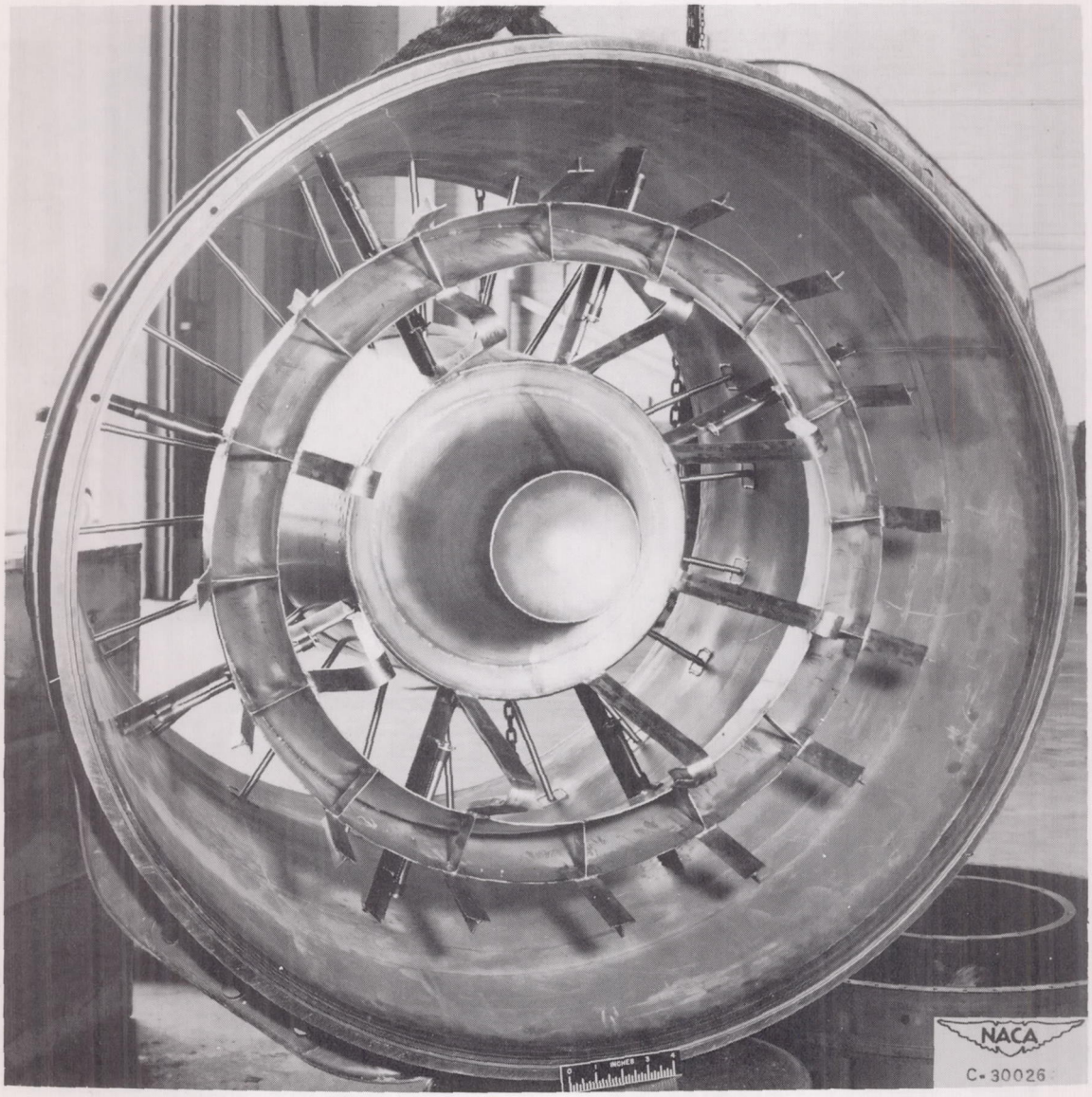

Figure 8. - View of diffuser F and flame holder E.

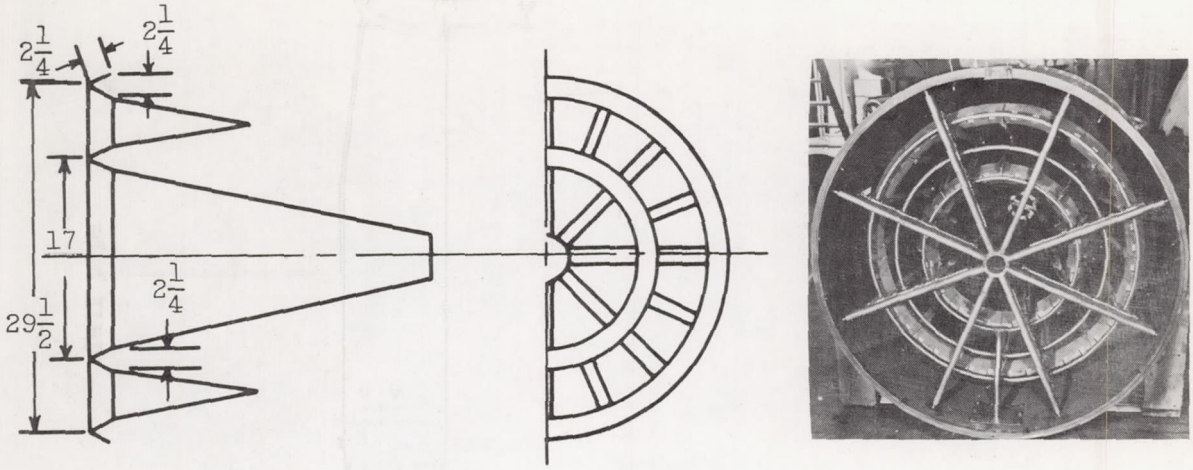

(a) Flame holder A; blockage, 41.3 percent.

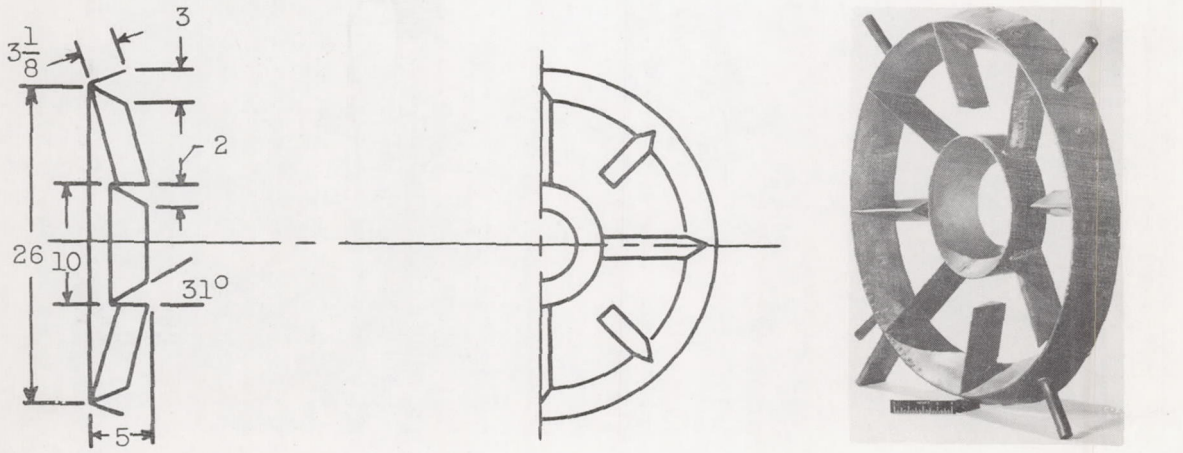

(b) Flame holder B; blockage, 33.9 percent.

NACA
C-29478
C-29862

Figure 9. - Details of flame holders investigated. All dimensions in inches.

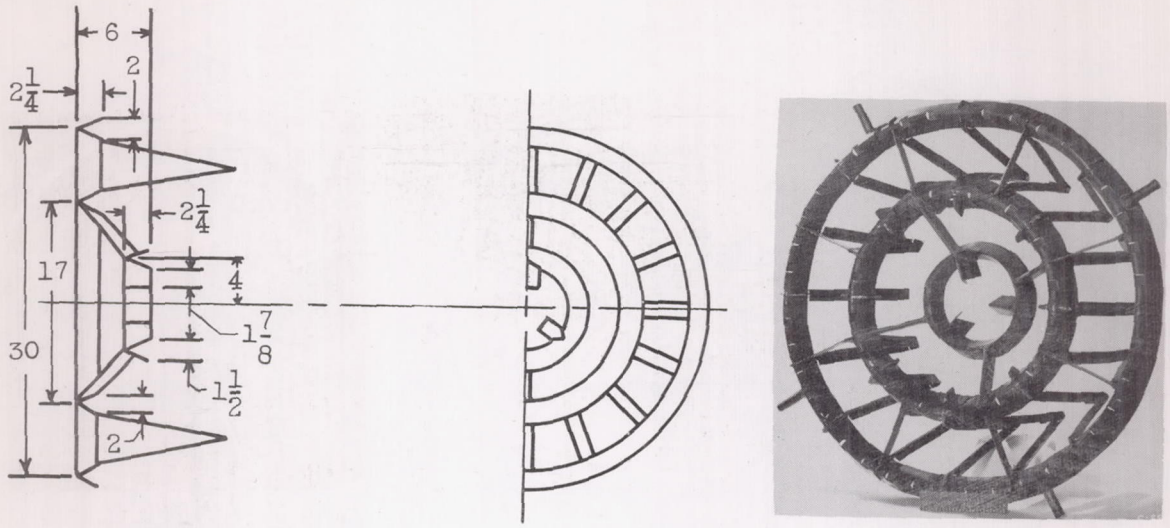

(c) Flame holder C; blockage, 40.6 percent.

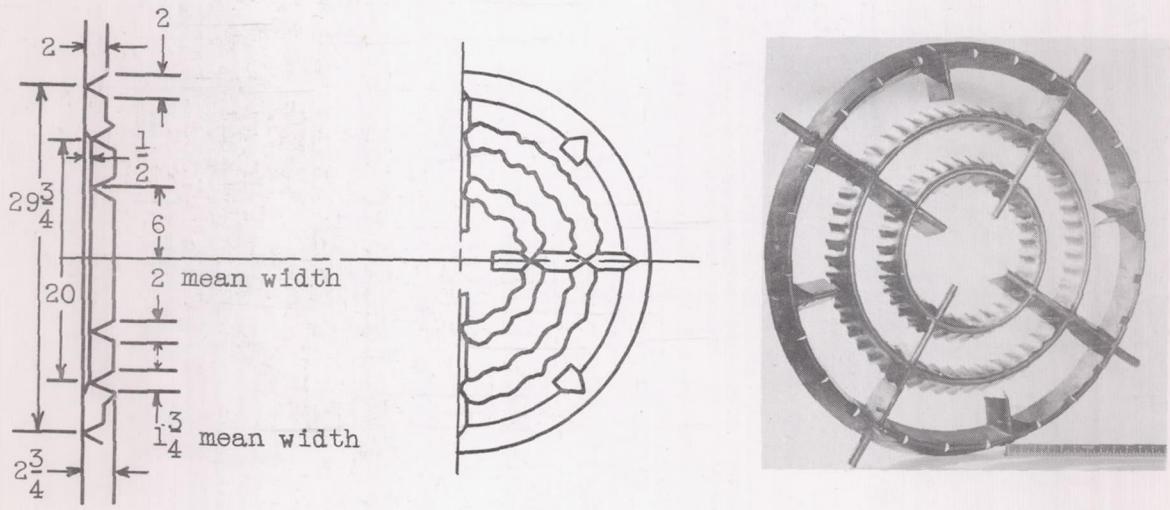

(d) Flame holder D; blockage, 40.5 percent.

NACA
C-29811
C-29813

Figure 9. - Concluded. Details of flame holders investigated. All dimensions in inches.

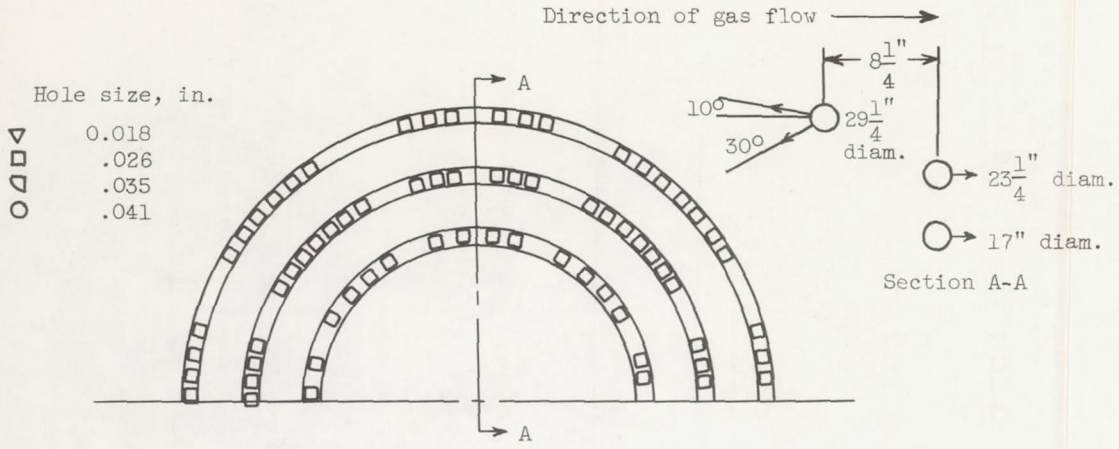

(a) Location of orifices in three-ring fuel manifold A.

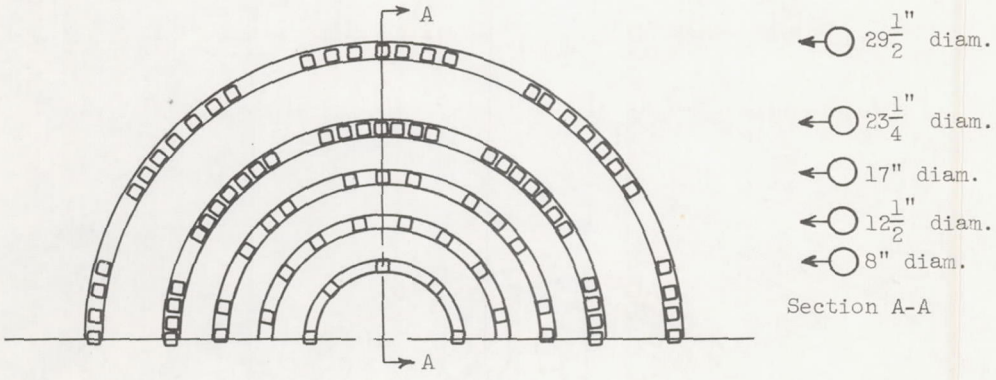

(b) Location of orifices in five-ring fuel manifold B.

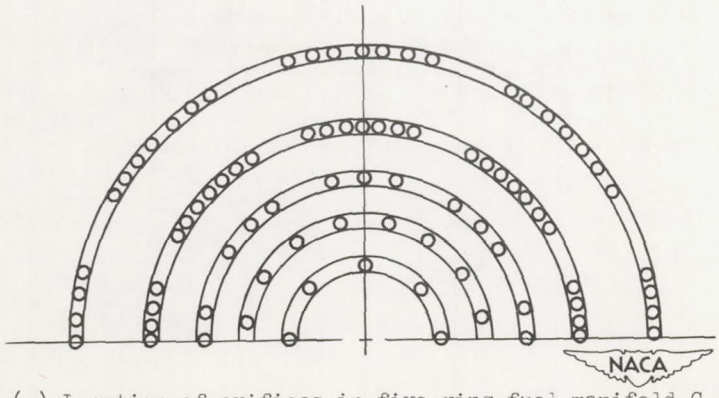

(c) Location of orifices in five-ring fuel manifold C. Dimensions and injection same as B.

Figure 10. - Fuel systems investigated.

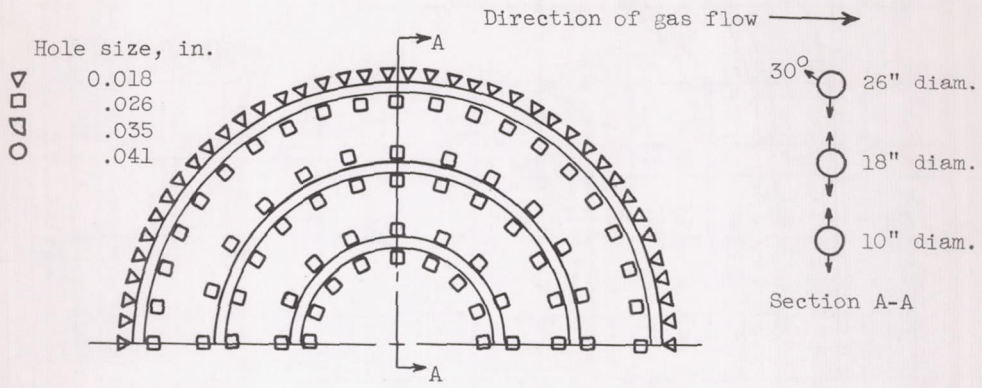

(d) Location of orifices in three-ring fuel manifold D.

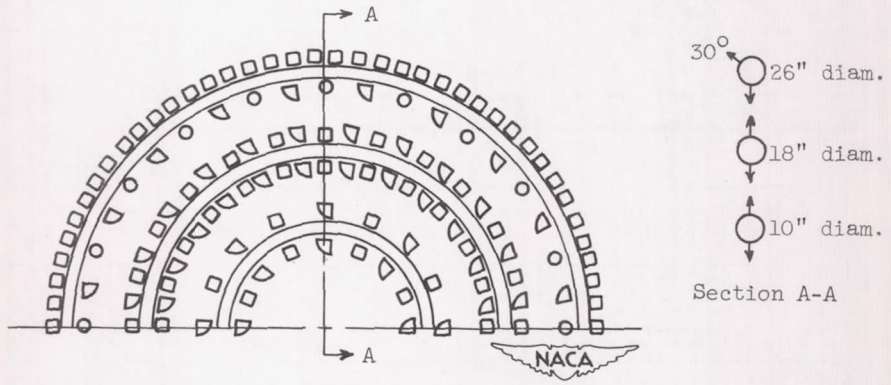

(e) Location of orifices in three-ring fuel manifold E.

Figure 10. - Continued. Fuel systems investigated.

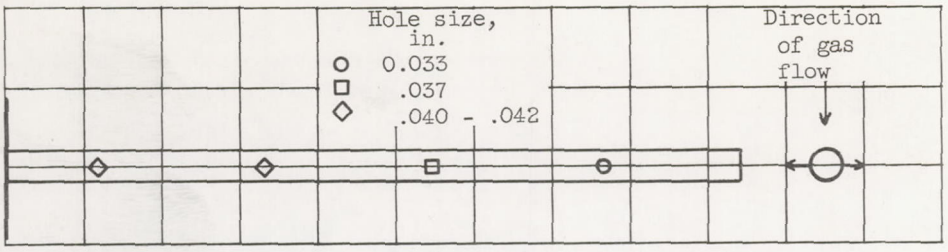

(f) Location of orifices in 20-spray-bar fuel system F.

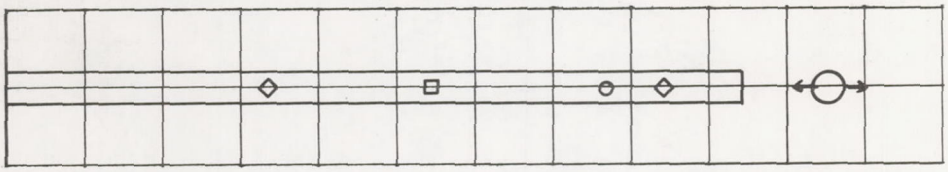

(g) Location of orifices in 10-spray-bar fuel system G.

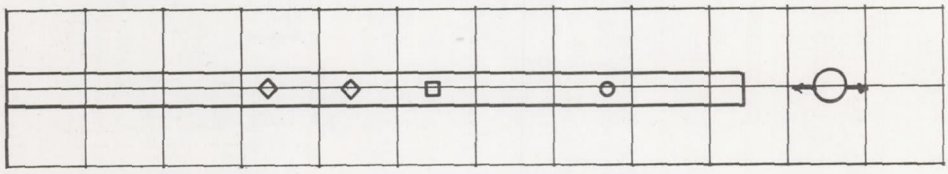

(h) Location of orifices in 10-spray-bar fuel system H.

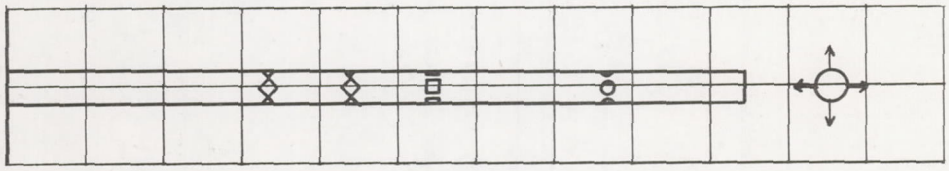

(i) Location of orifices in 10-spray-bar fuel system I.

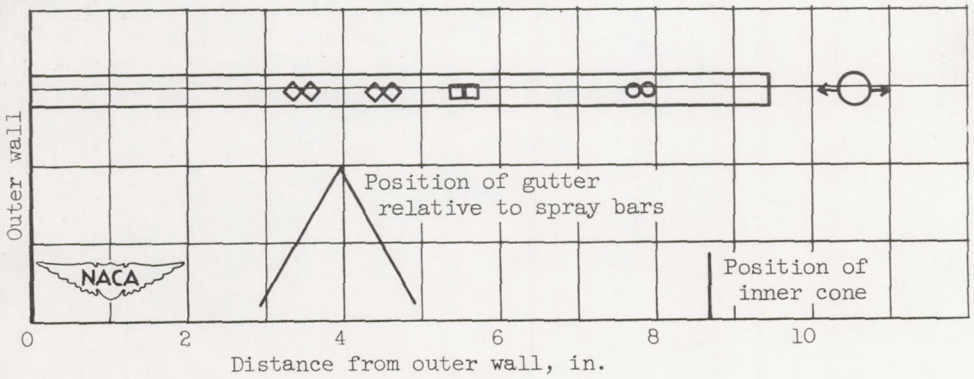

(j) Location of orifices in 10-spray-bar fuel system J.

Figure 10. - Concluded. Fuel systems investigated.

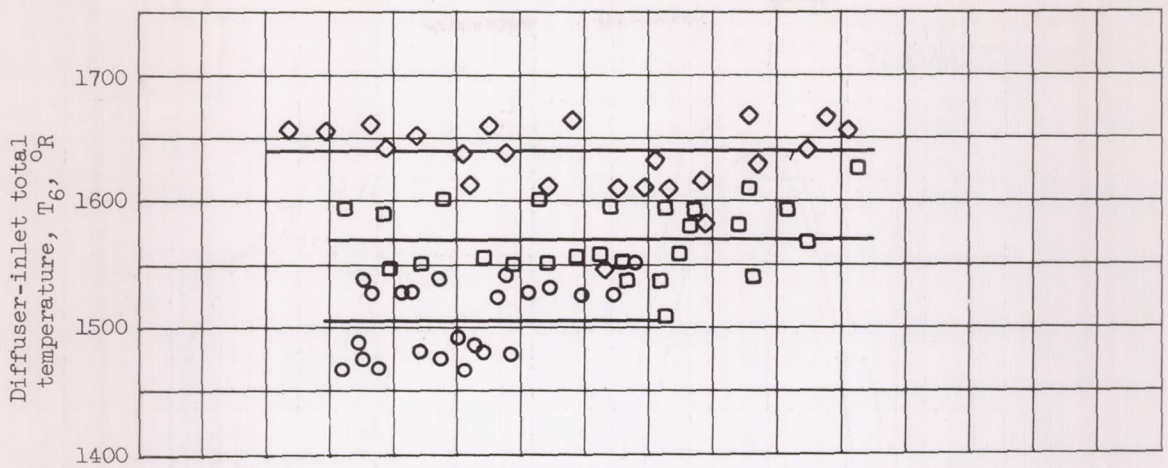

(a) Diffuser-inlet total temperature.

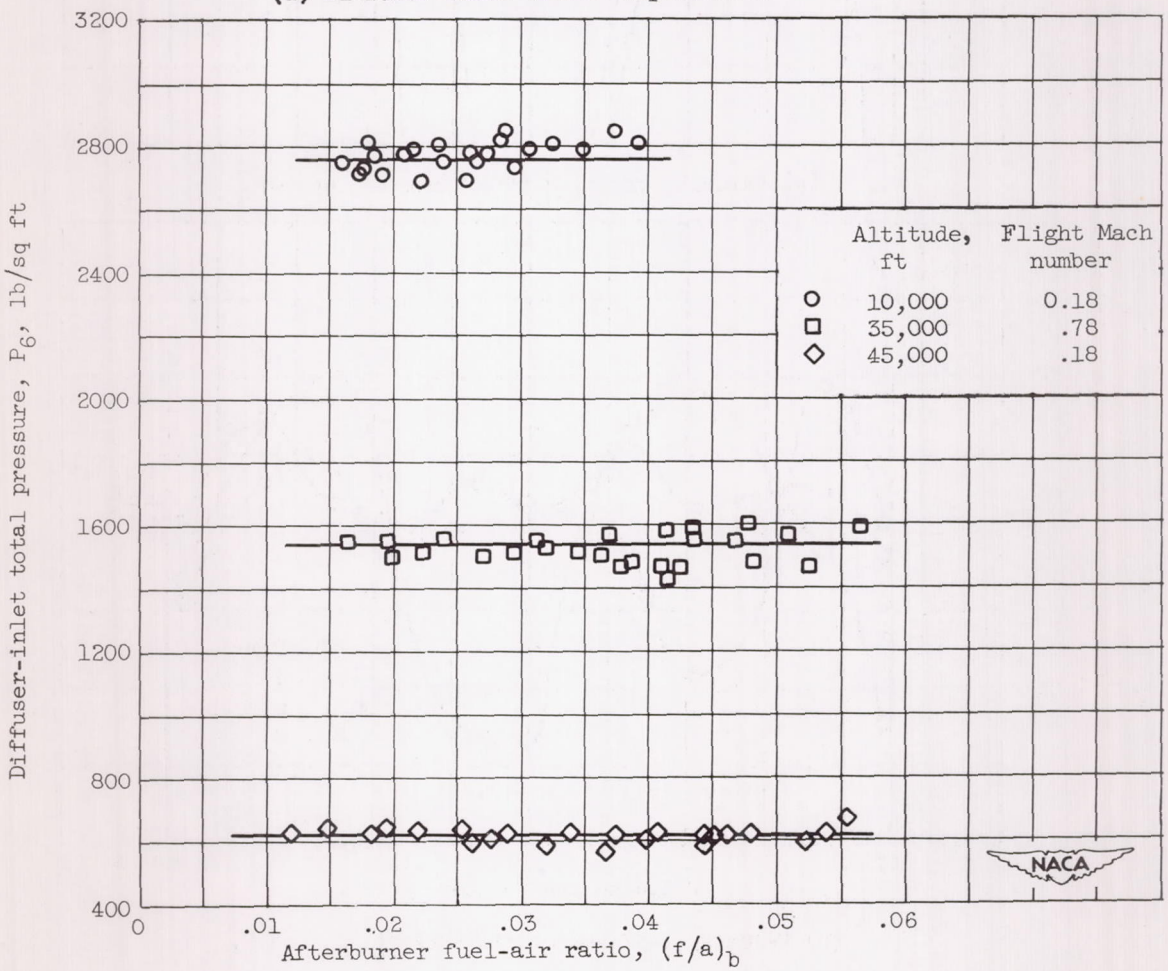

(b) Diffuser-inlet total pressure.

Figure 11. - Average diffuser-inlet conditions.

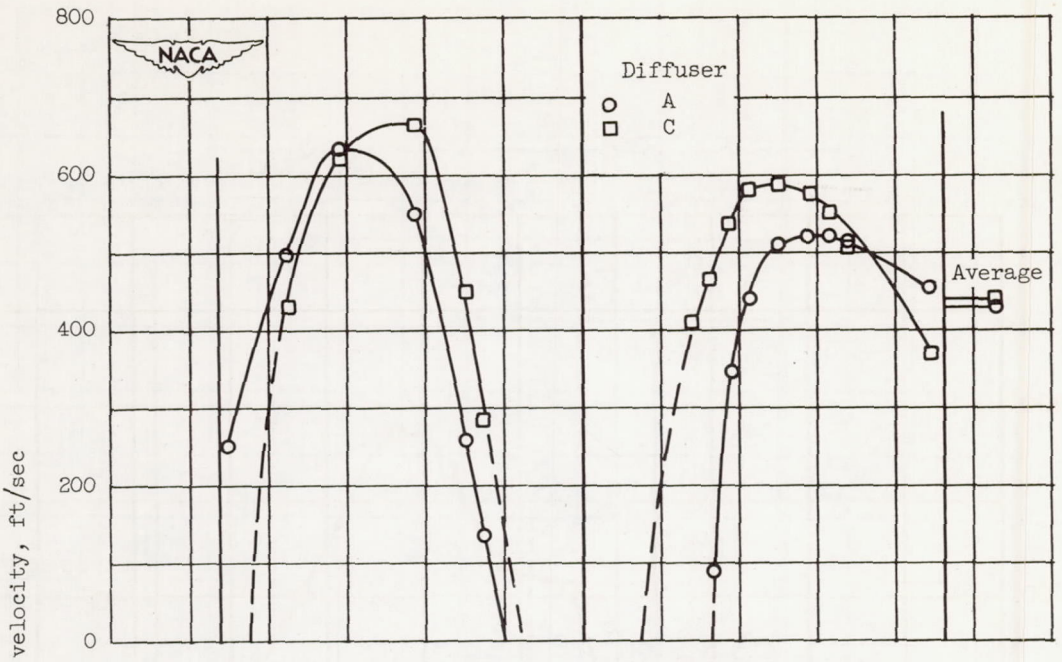

(a) Velocity profiles of diffusers A and C.

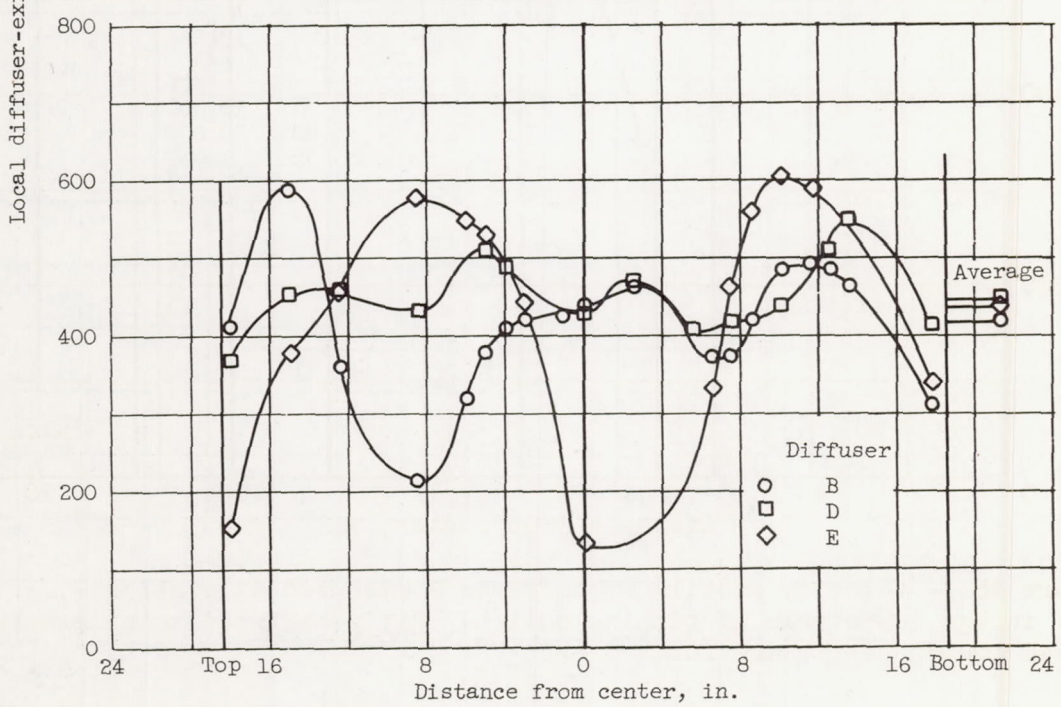

(b) Velocity profiles of diffusers B, D, and E.

Figure 12. - Velocity profiles of diffusers A to E measured at station 7, $42\frac{1}{2}$ inches downstream of turbine outlet. Diffuser-inlet total pressure, 1540 pounds per square foot.

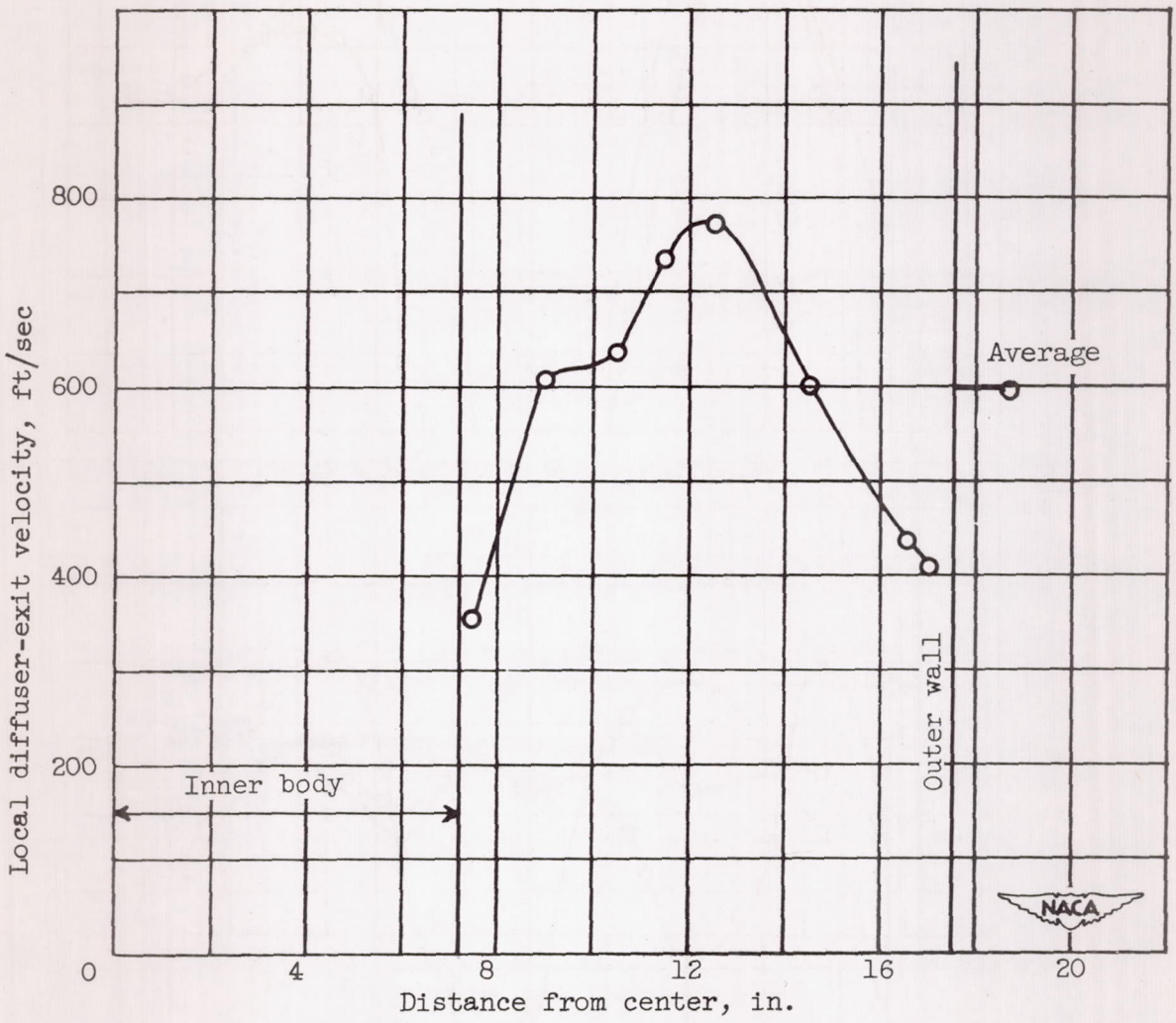

Figure 13. - Velocity profile of diffuser F measured at station 7, 31 inches downstream of turbine outlet. Diffuser-inlet total pressure, 1540 pounds per square foot.

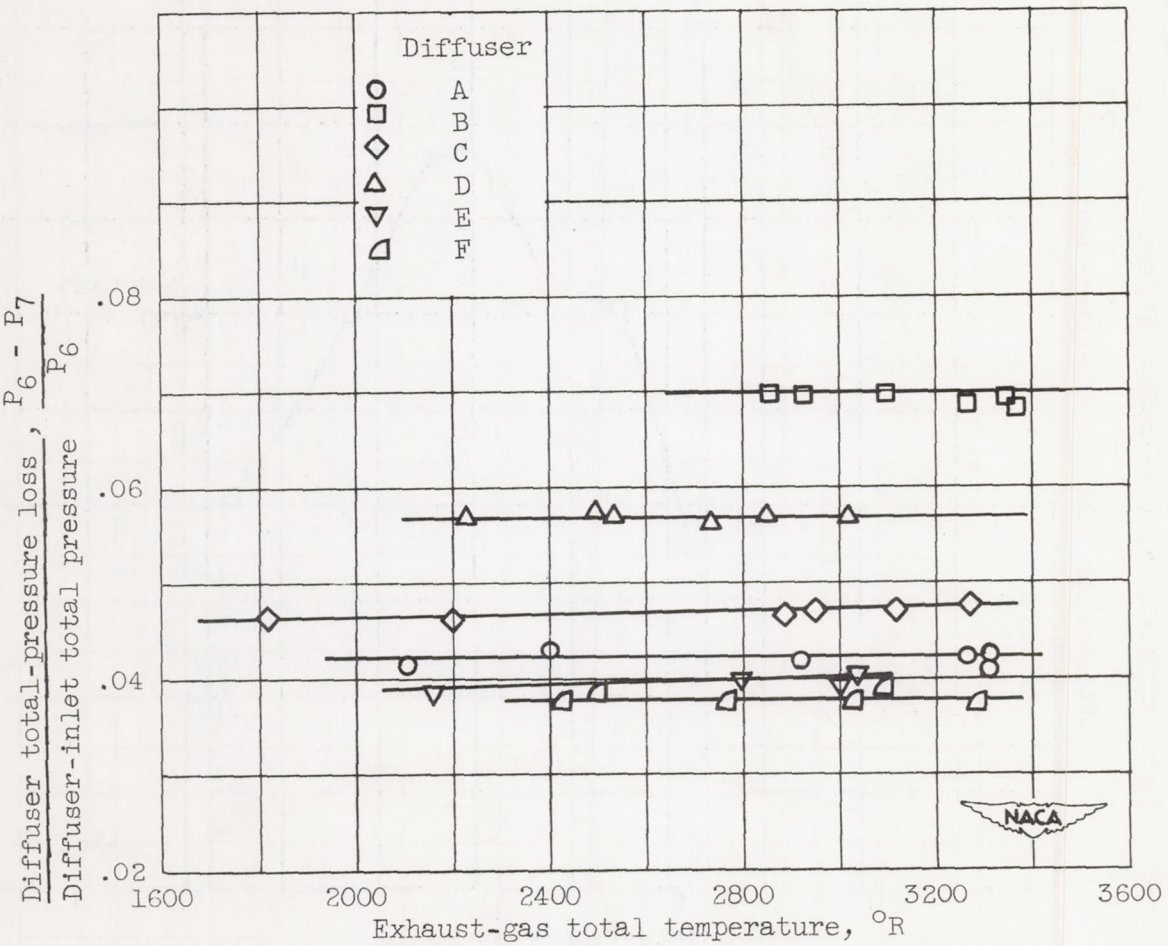

Figure 14. - Effect of diffuser design on diffuser total-pressure loss. Diffuser-inlet pressure, 1540 pounds per square foot.

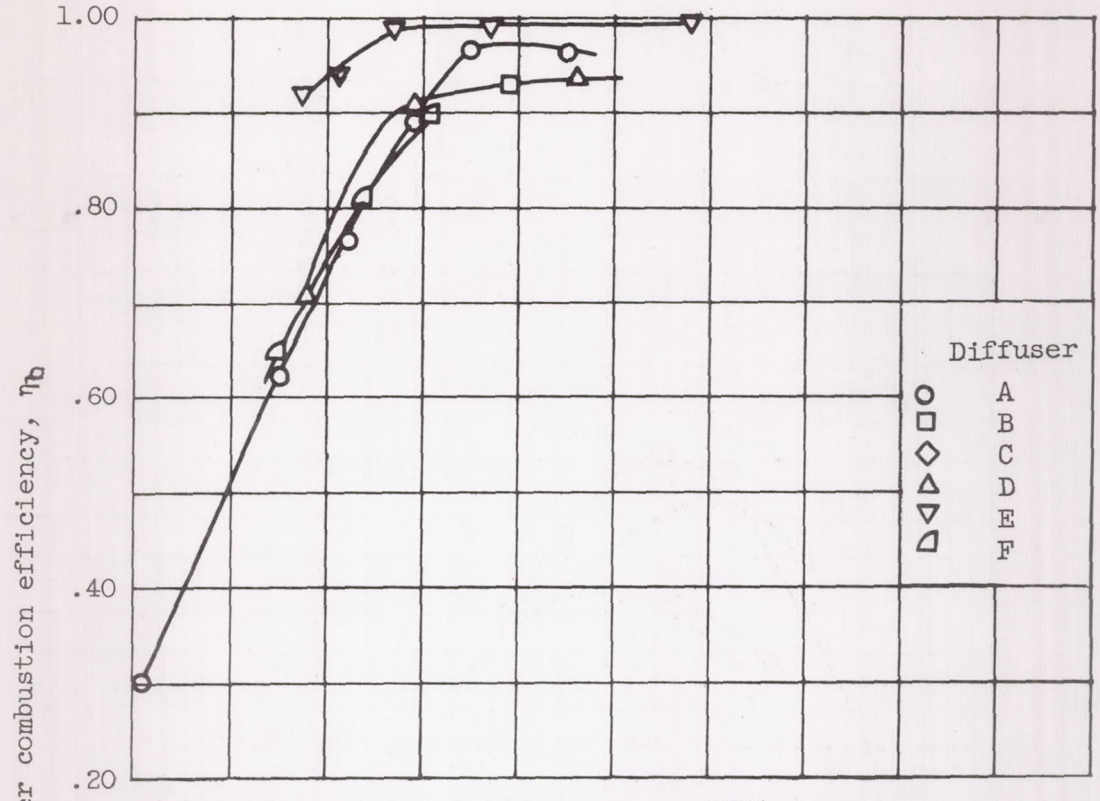

(a) Diffuser-inlet total pressure, 2750 pounds per square foot.

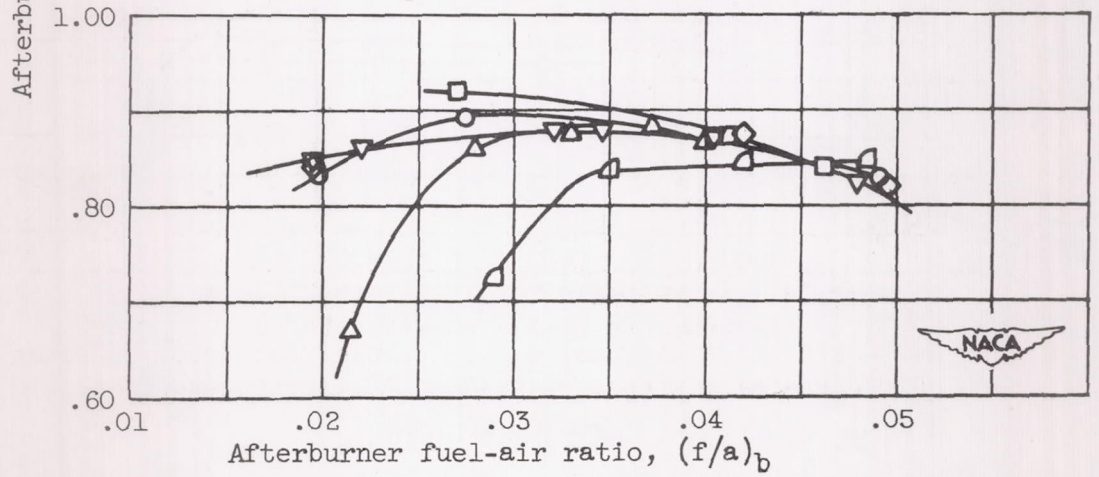

(b) Diffuser-inlet total pressure, 1540 pounds per square foot.

Figure 15. - Effect of velocity profile on afterburner combustion efficiency.

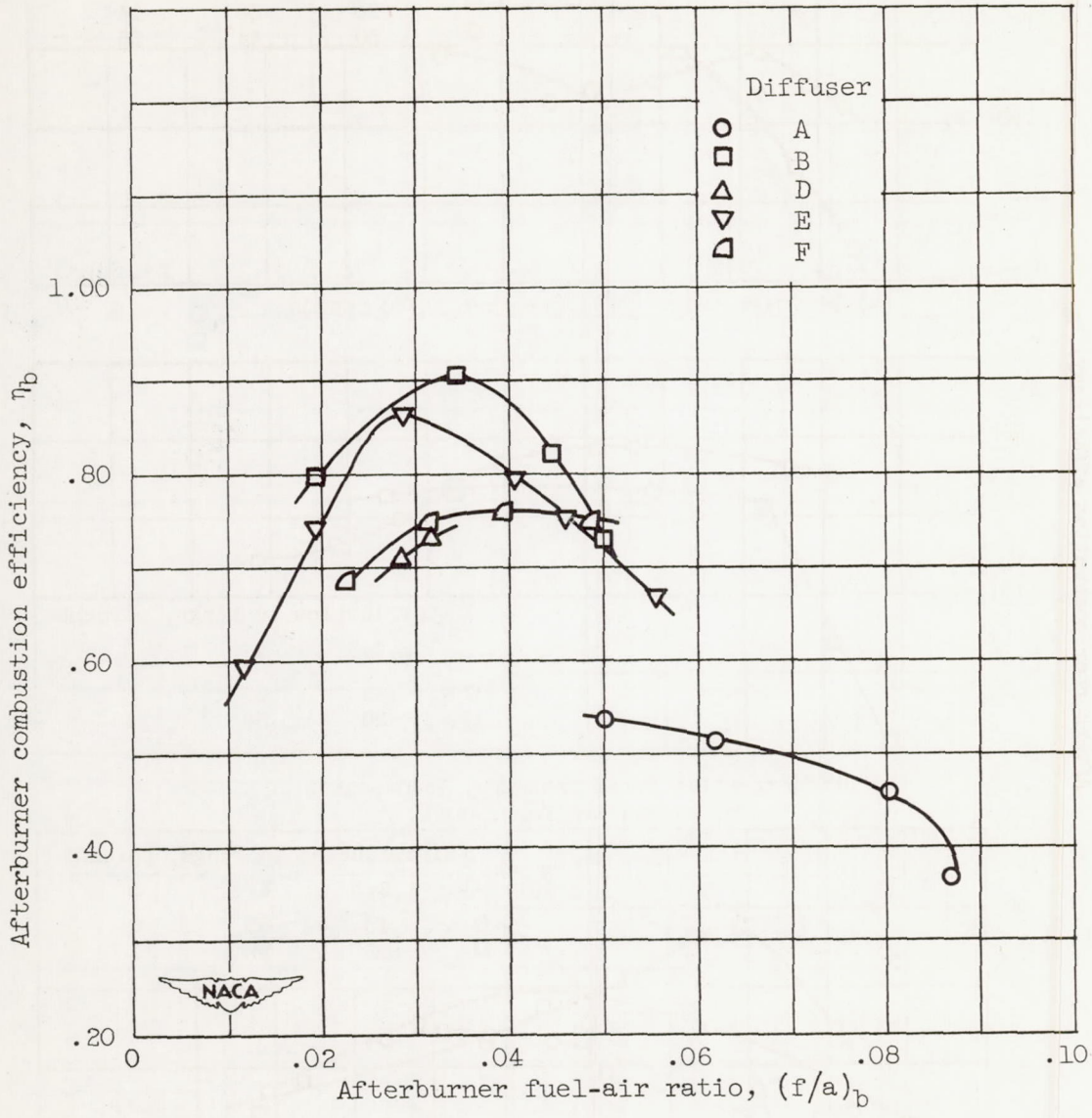

(c) Diffuser-inlet total pressure, 620 pounds per square foot.

Figure 15. - Concluded. Effect of velocity profile on afterburner combustion efficiency.

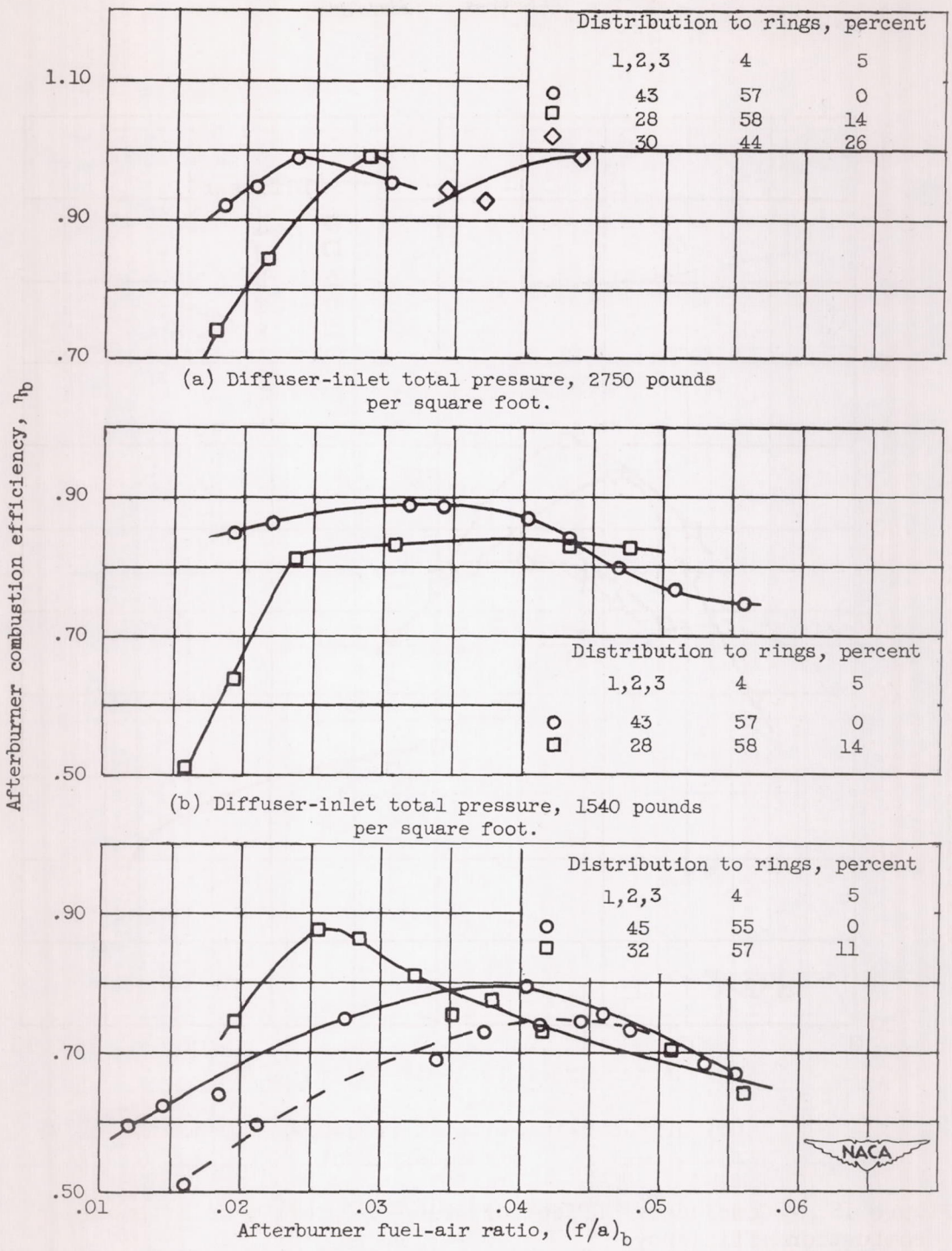

Figure 16. - Effect of fuel distribution on combustion efficiency. Configuration E1.

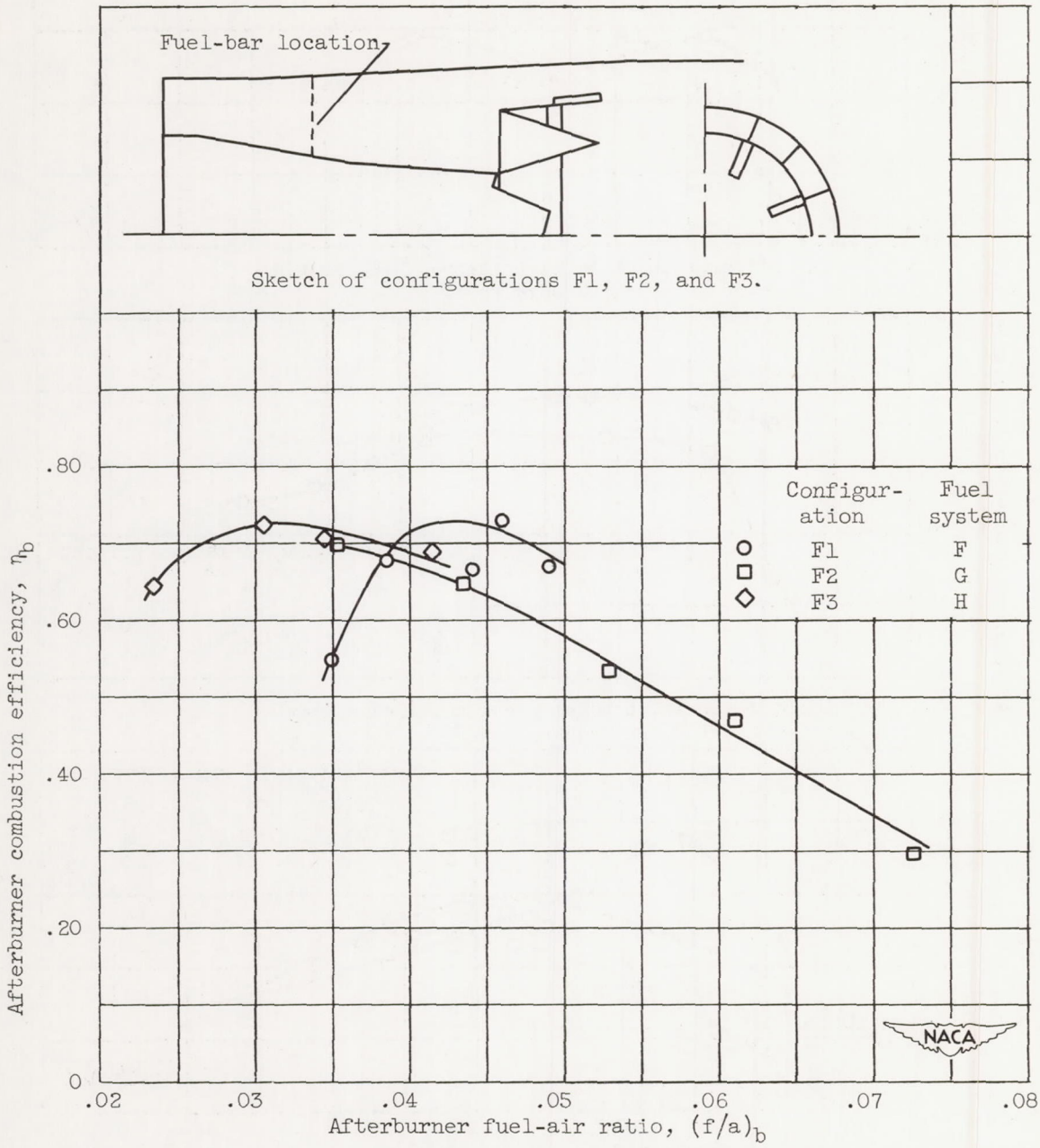

Figure 17. - Effect of radial fuel distribution on performance. Diffuser-inlet total pressure, 620 pounds per square foot.

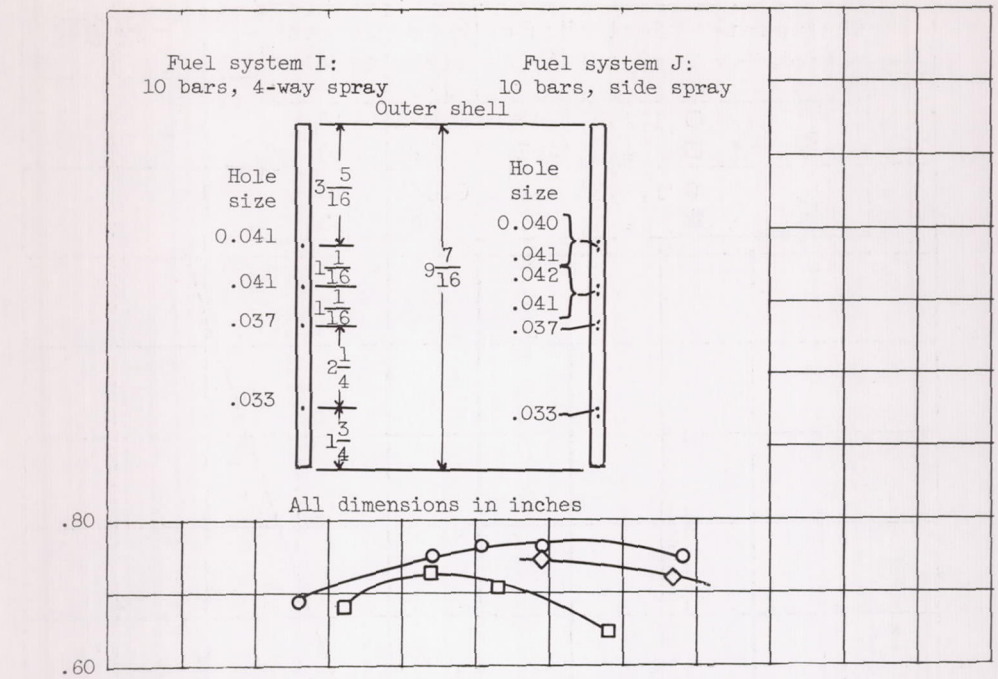

(a) Diffuser-inlet total pressure, 620 pounds per square foot.

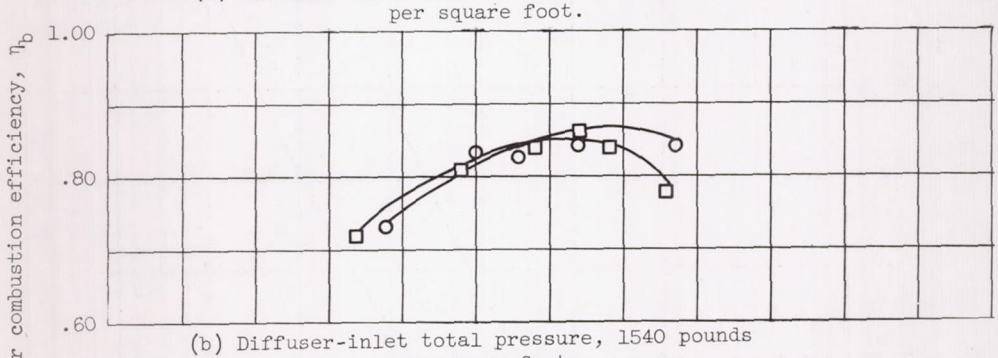

(b) Diffuser-inlet total pressure, 1540 pounds per square foot.

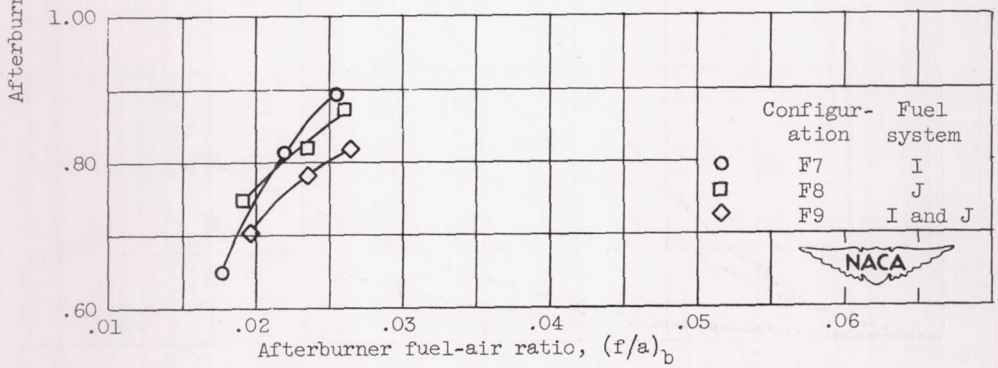

(c) Diffuser-inlet total pressure, 2750 pounds per square foot.

Figure 18. - Effect of circumferential fuel distribution on performance.

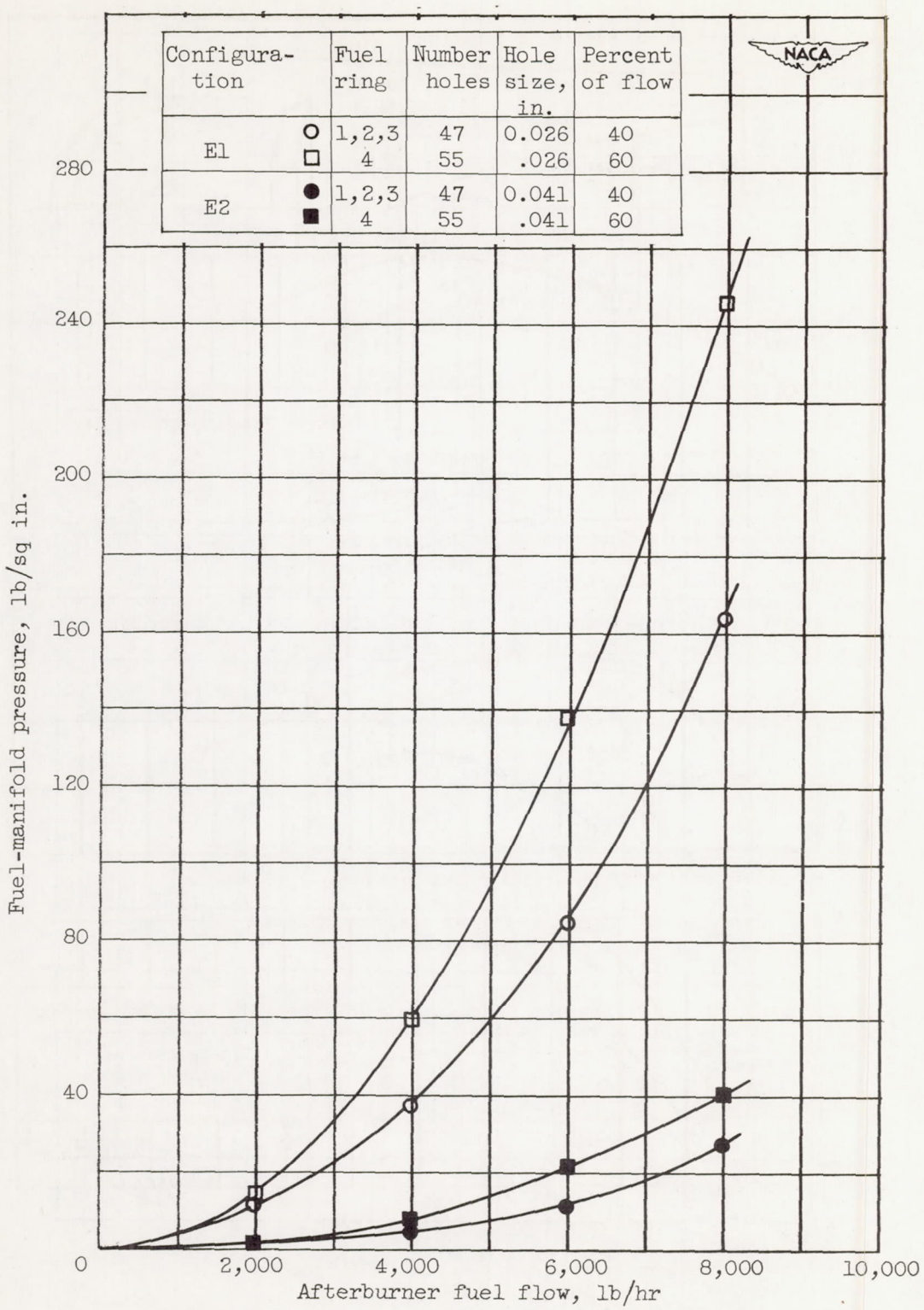

Figure 19. - Effect of hole size on fuel-manifold pressure.

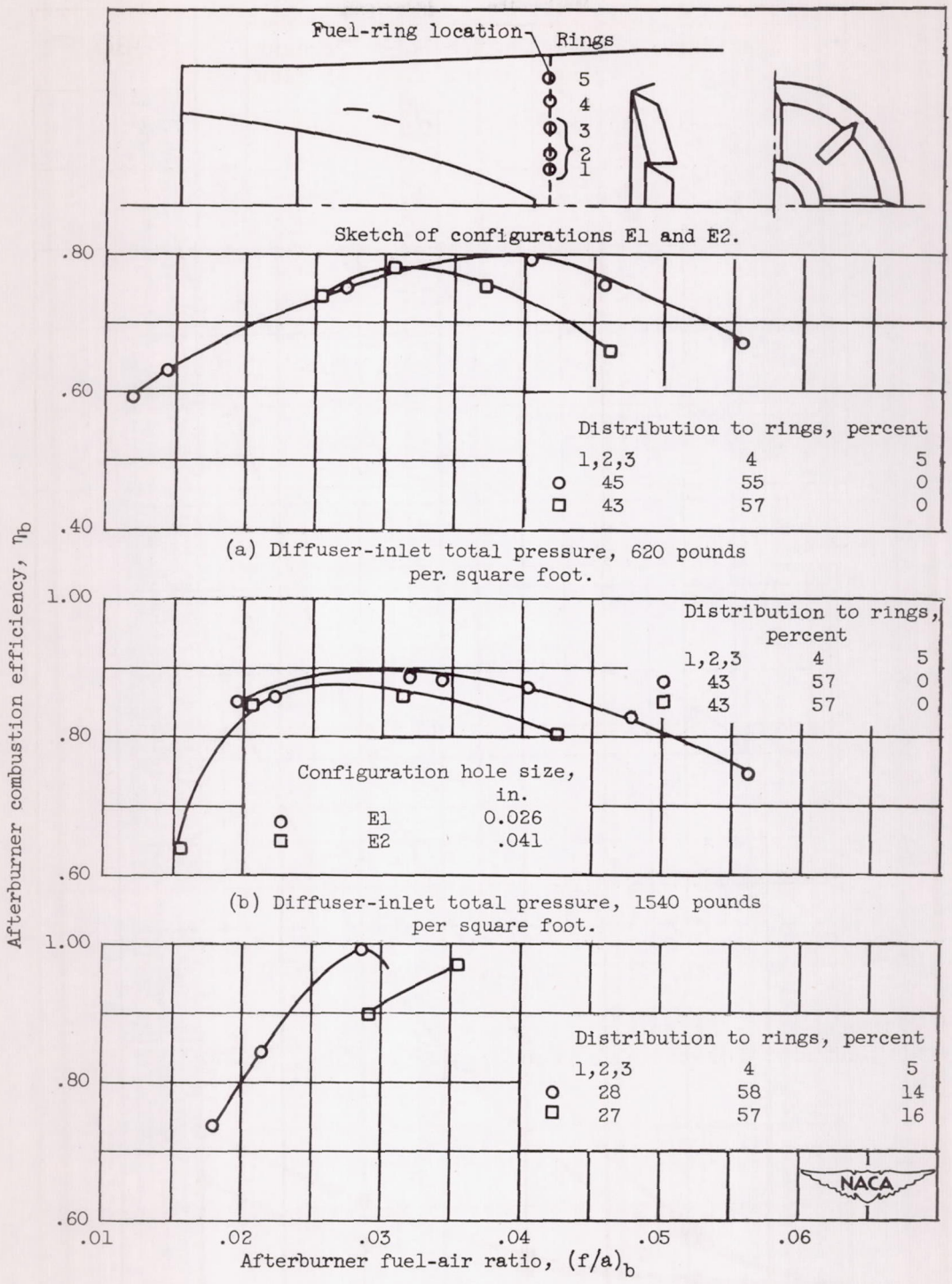

Figure 20. - Effect of fuel pressure (hole size) on performance. Five-ring fuel manifold upstream injection.

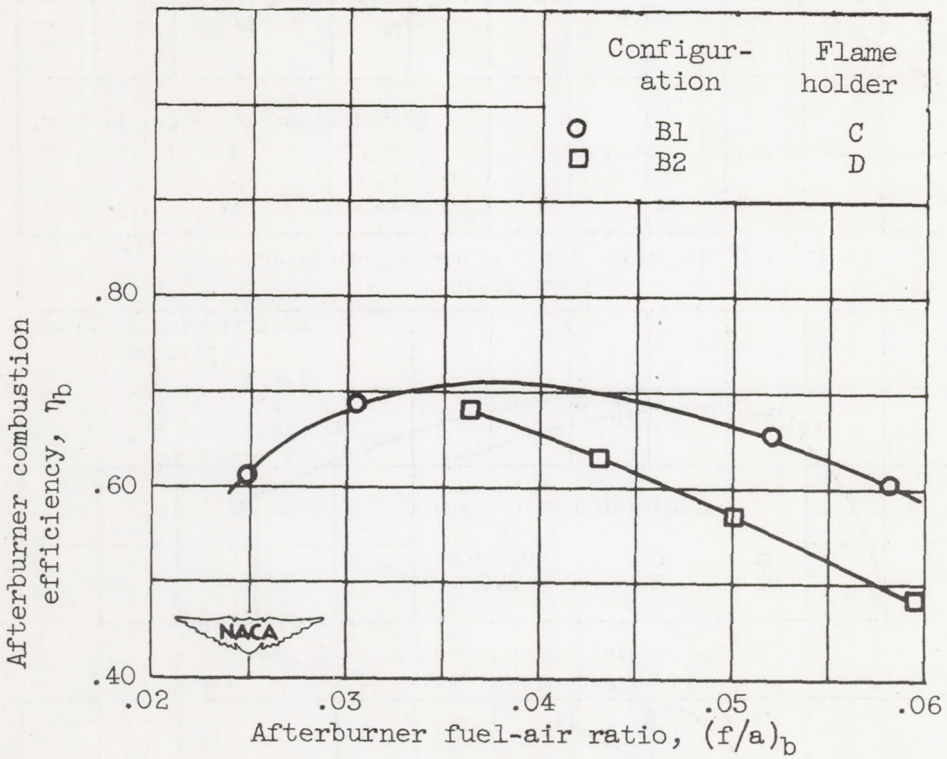

Figure 21. - Effect of flame-holder design on performance. Diffuser-inlet total pressure, 620 pounds per square foot.

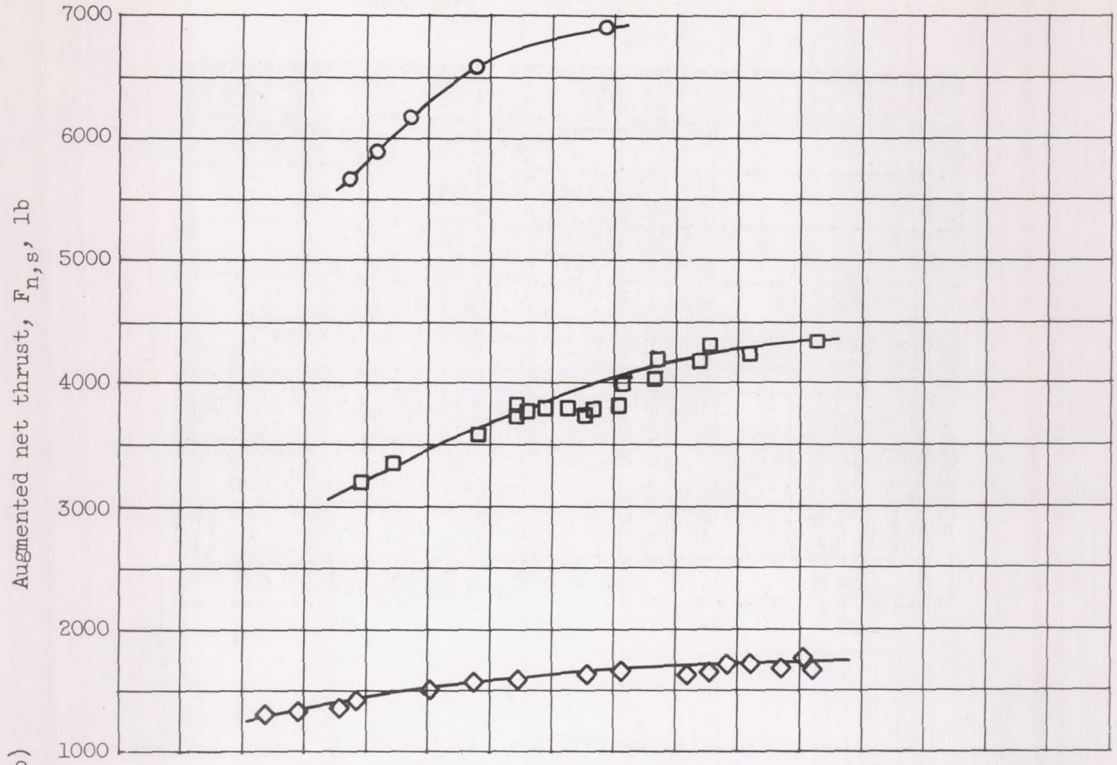

(a) Augmented net thrust.

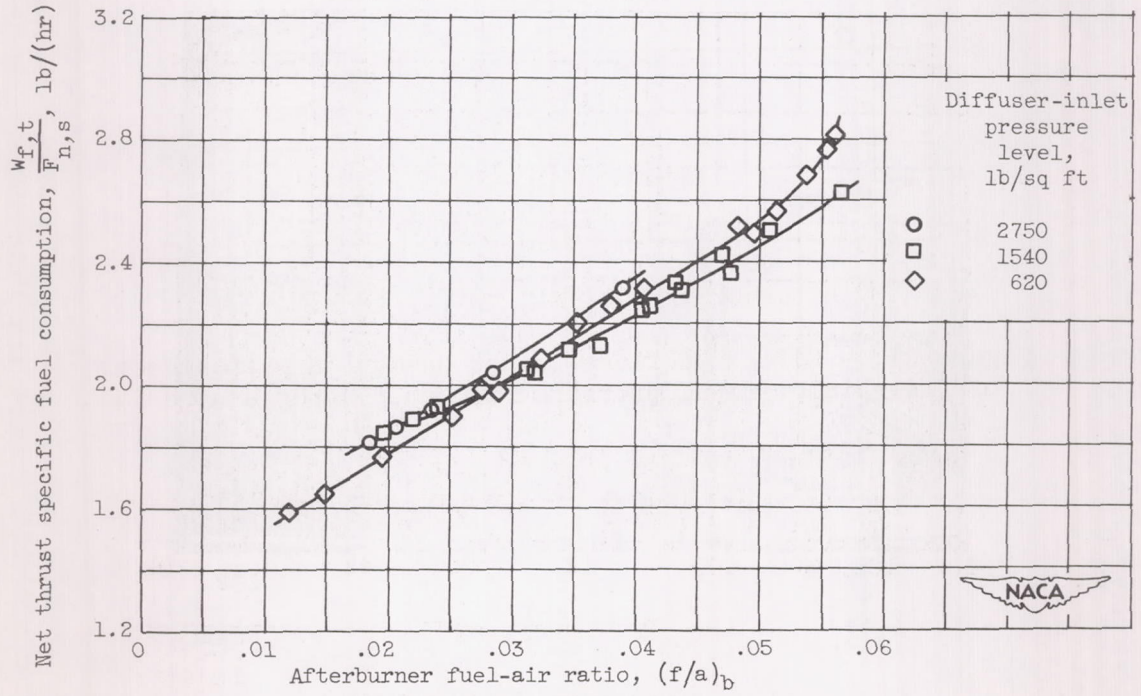

(b) Specific fuel consumption.

Figure 22. - Performance of afterburner configuration E1.

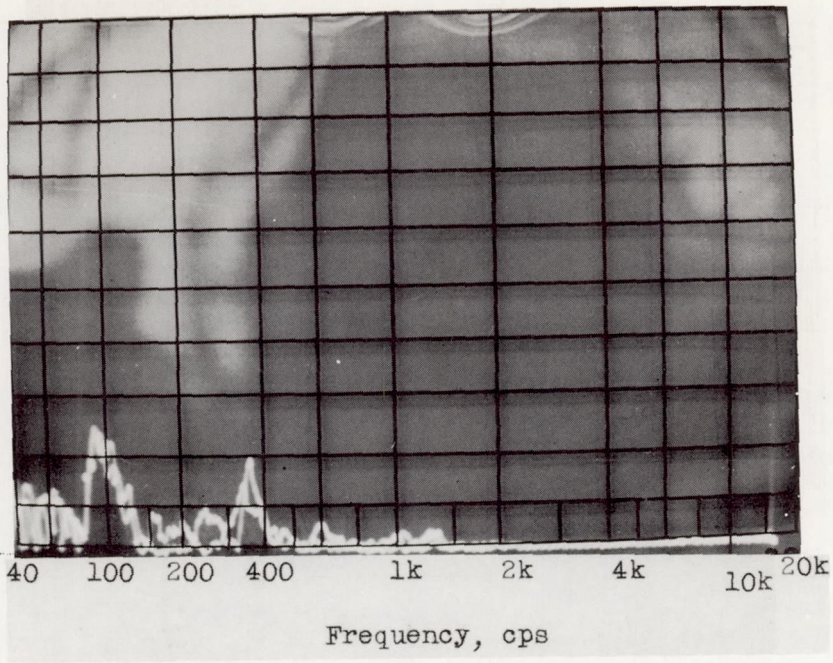

(a) Afterburner operation without screech.

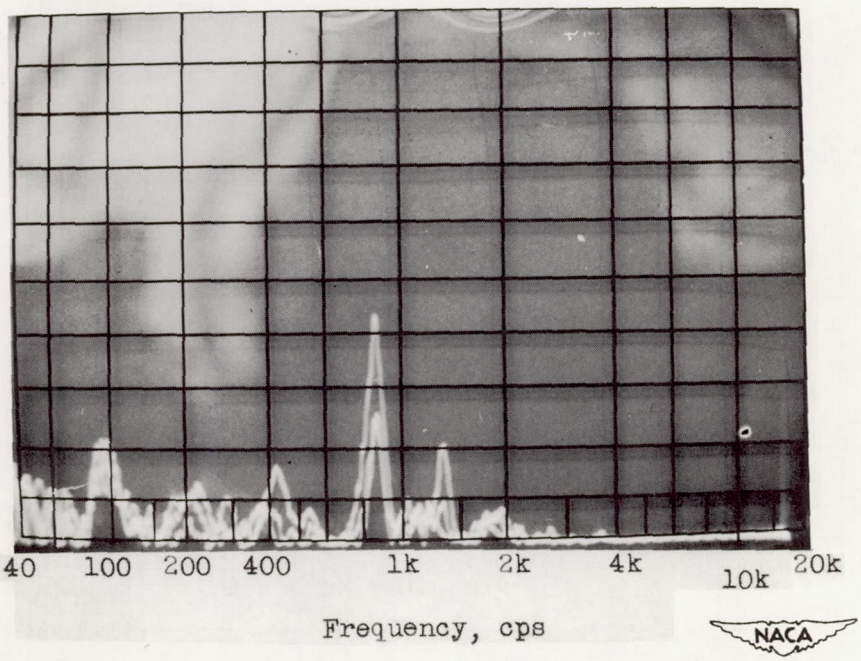

(b) Afterburner operation with screech.

Figure 23. - Examples of pressure pulsations with and without screech.

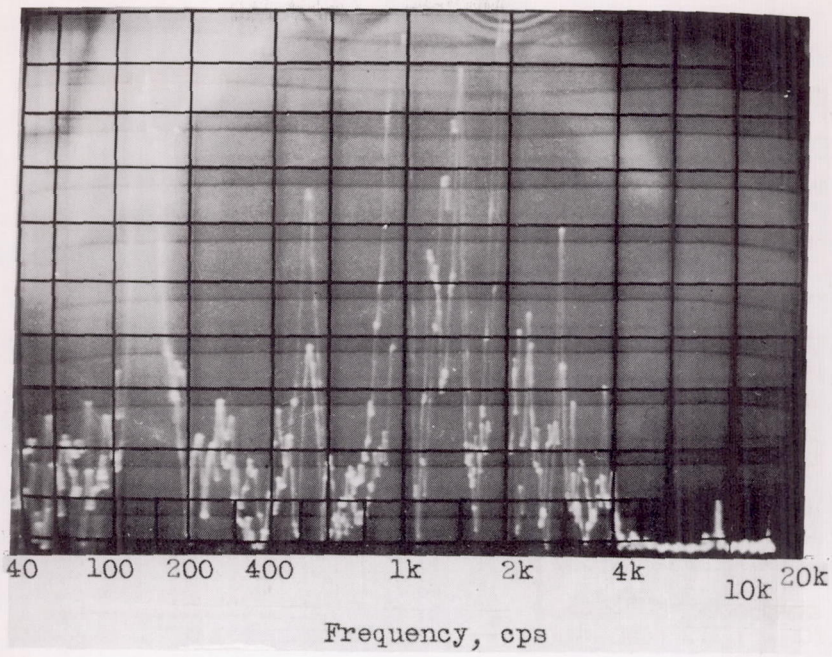

(c) Typical frequency distribution with screech.

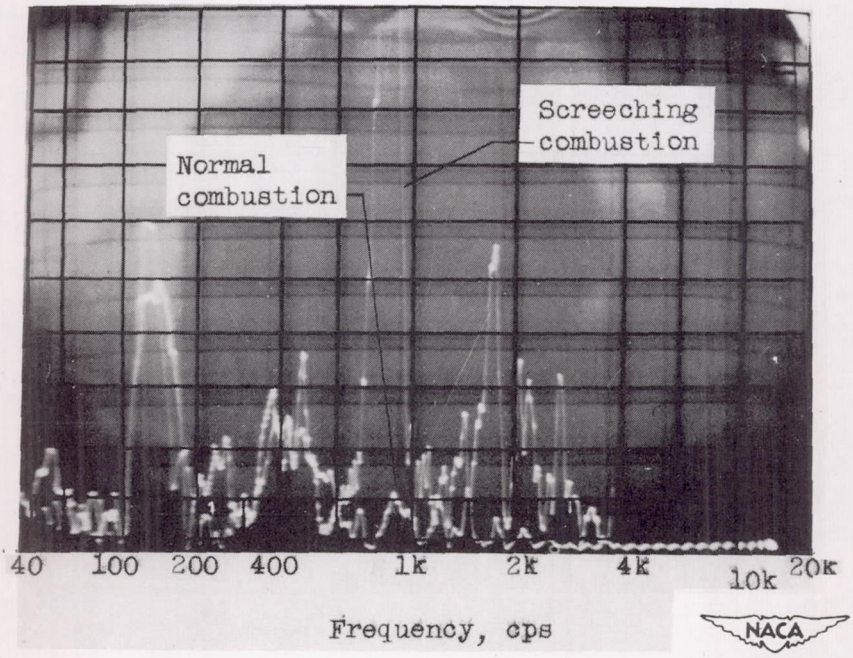

(d) Harmonic distribution with screech (also no-screech trace superimposed).

Figure 23. - Concluded. Examples of pressure pulsations with and without screech.

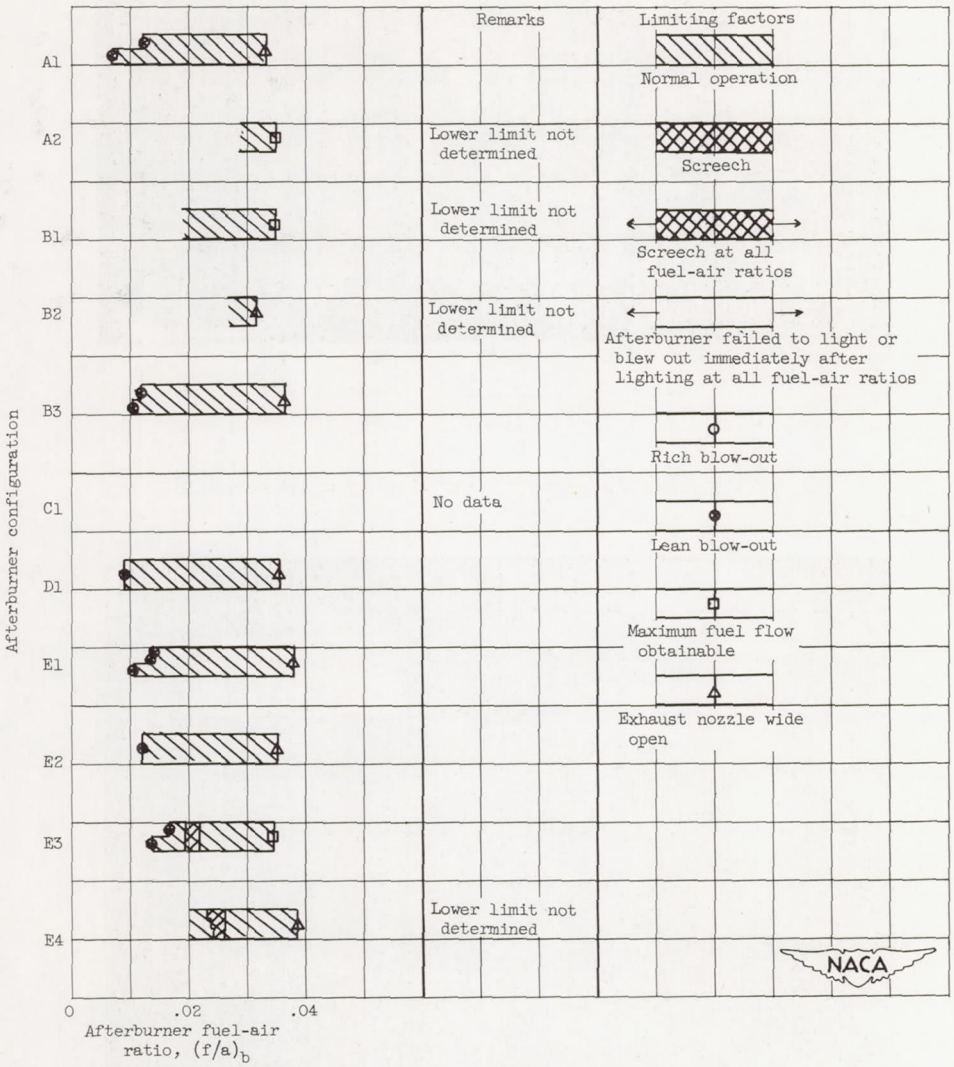

(a) Diffuser-inlet total pressure, 2750 pounds per square foot.

Figure 24. - Operational characteristics of configurations.

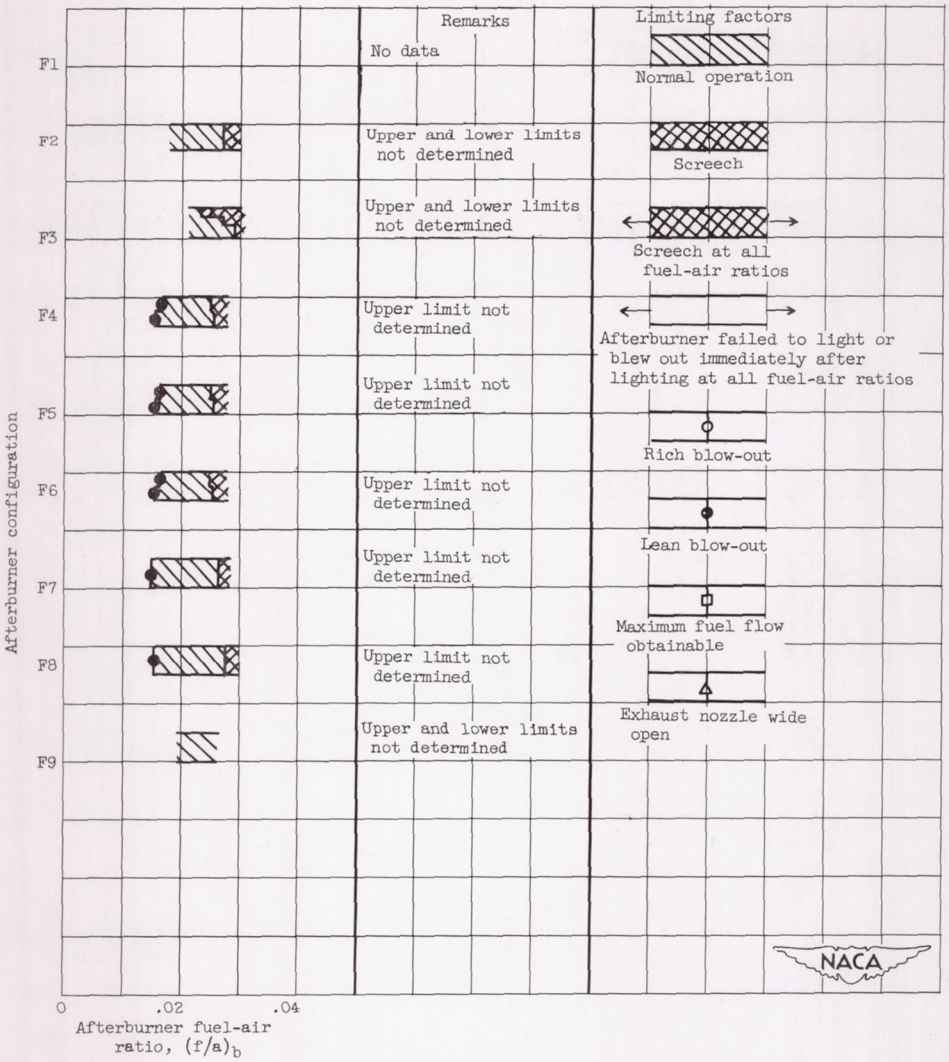

(a) Concluded. Diffuser-inlet total pressure, 2750 pounds per square foot.

Figure 24. - Continued. Operational characteristics of configurations.

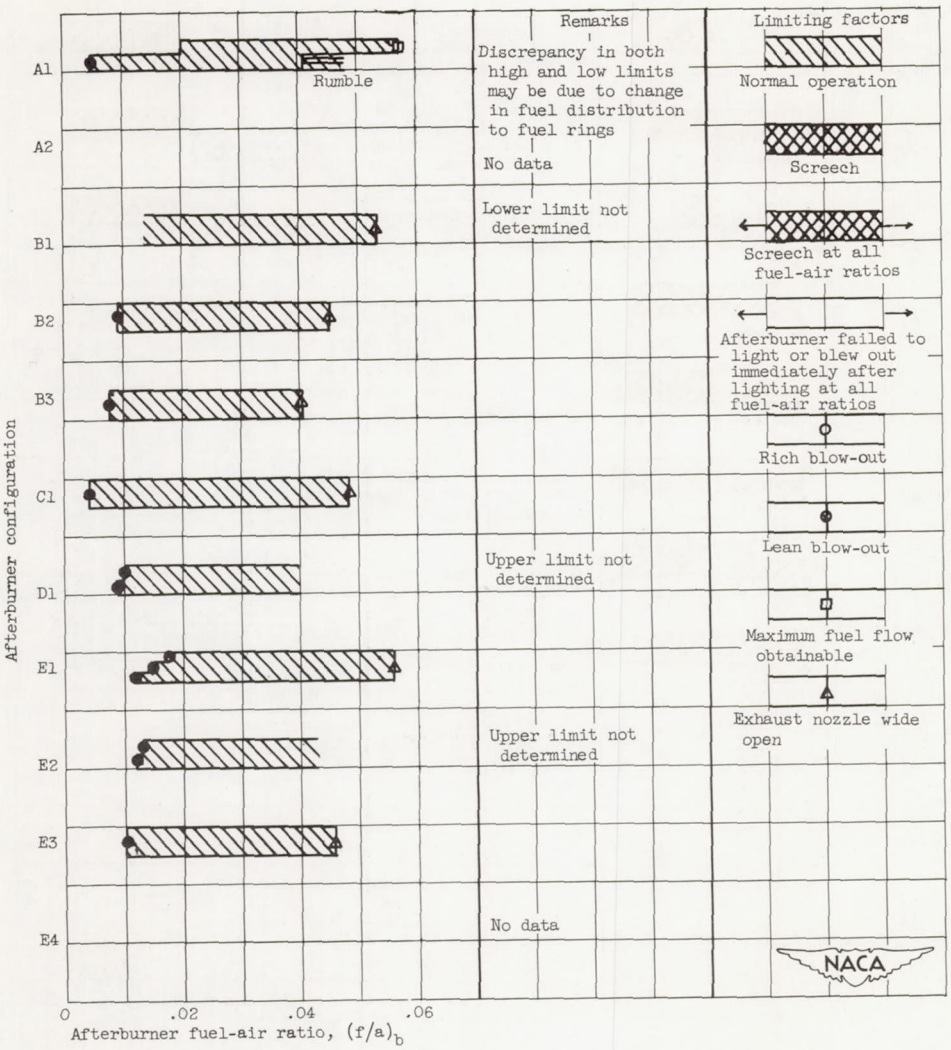

(b) Diffuser-inlet total pressure, 1540 pounds per square foot.

Figure 24. - Continued. Operational characteristics of configurations.

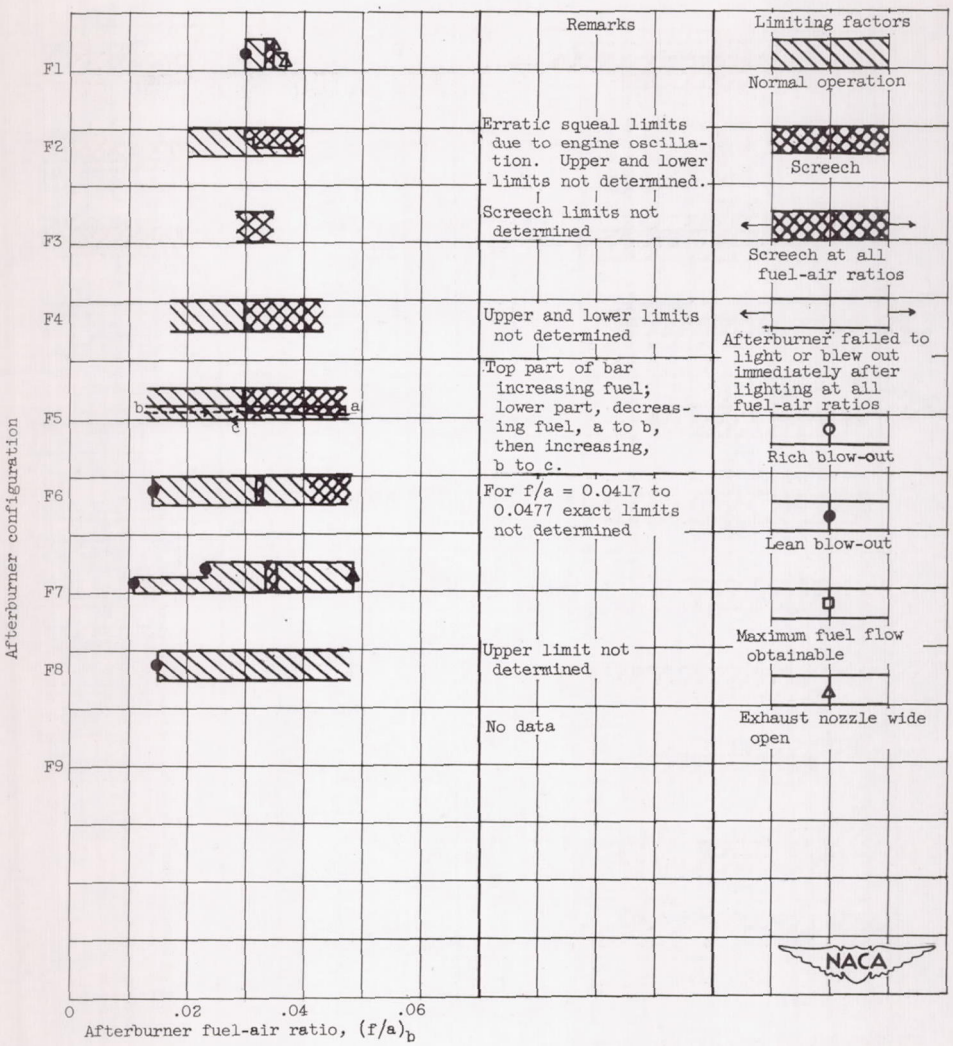

(b) Concluded. Diffuser-inlet total pressure, 1540 pounds per square foot.

Figure 24. - Continued. Operational characteristics of configurations.

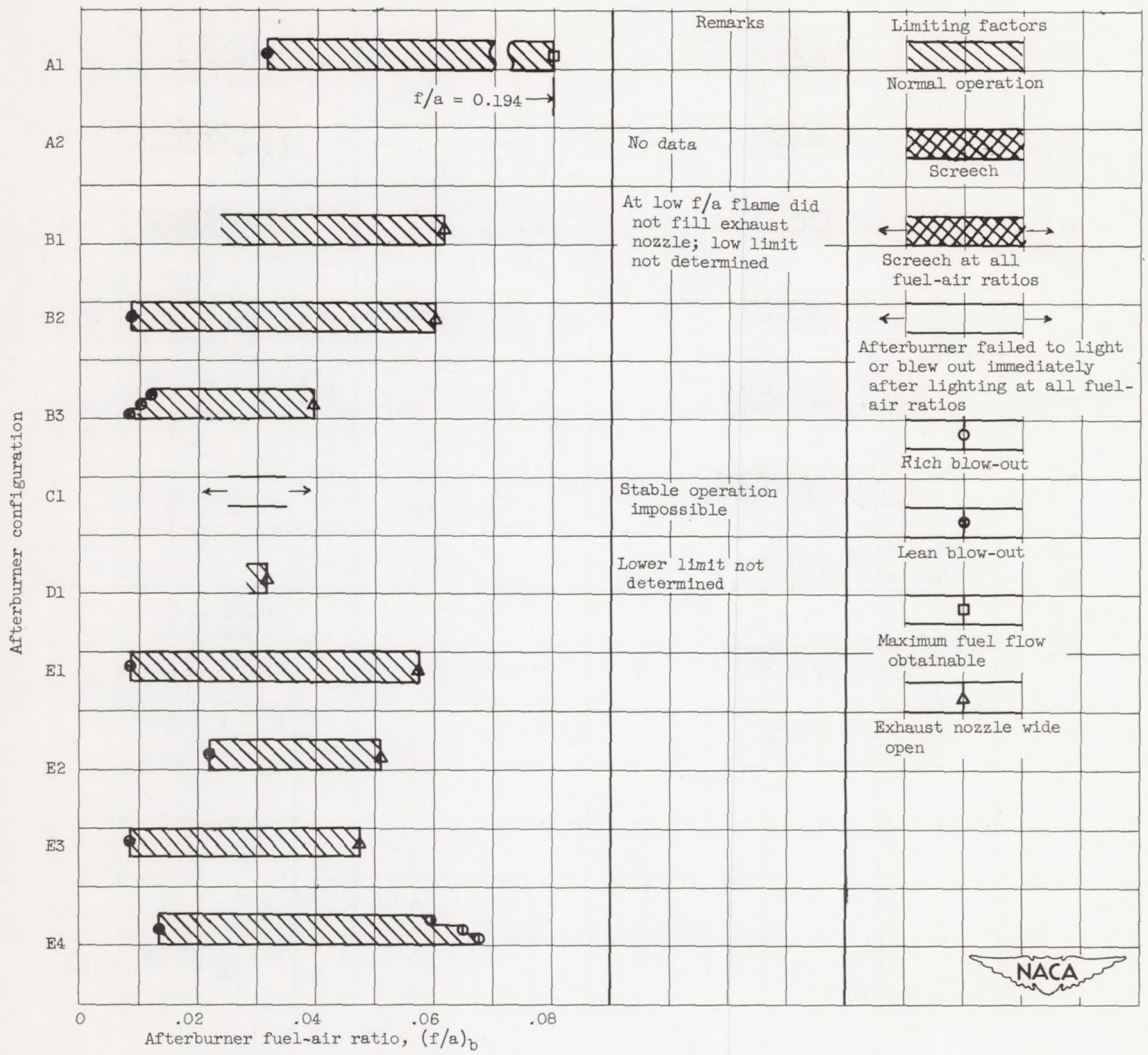

(c) Diffuser-inlet total pressure, 620 pounds per square foot.

Figure 24. - Continued. Operational characteristics of configurations.

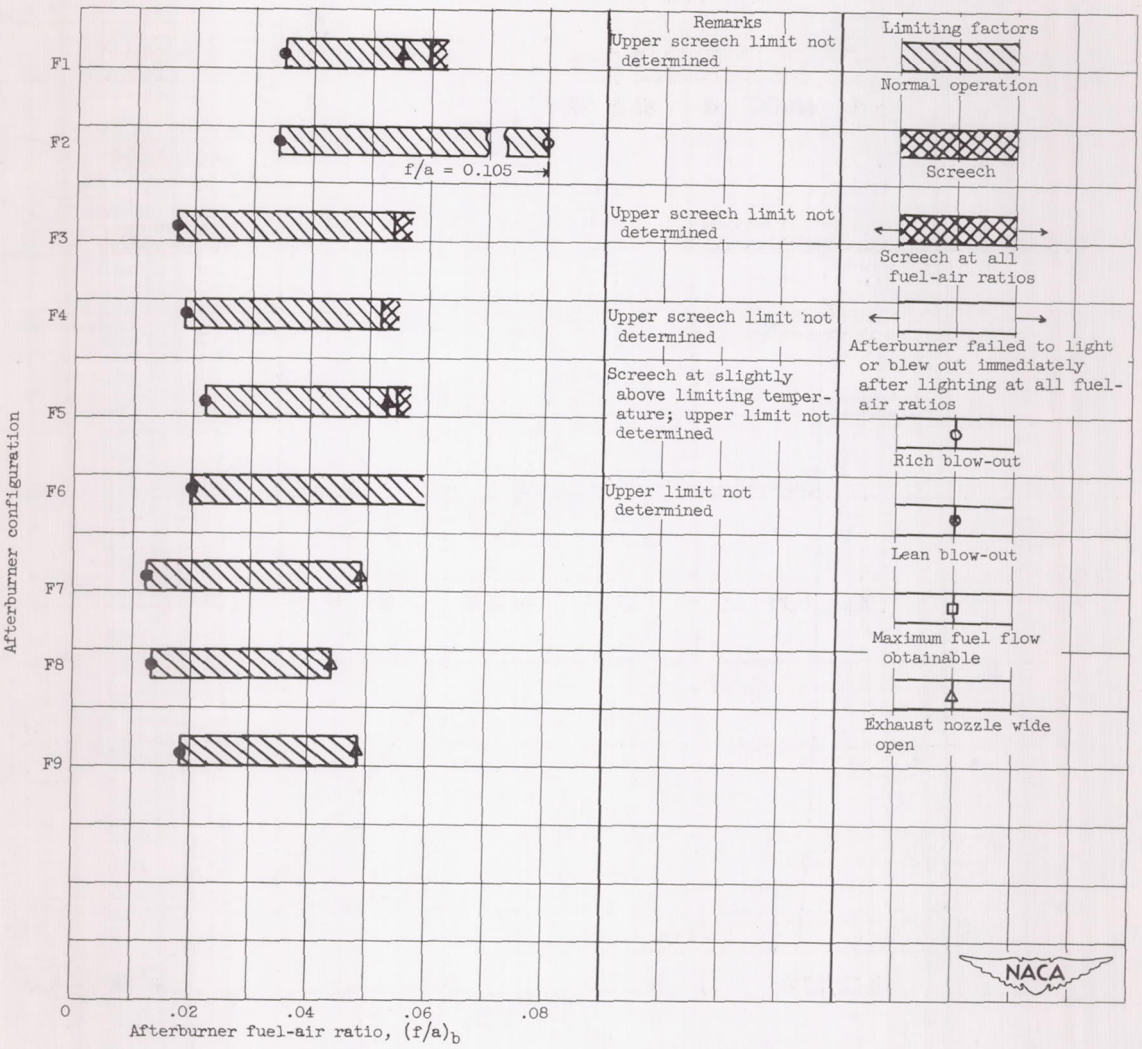

(c) Concluded. Diffuser-inlet total pressure, 620 pounds per square foot.

Figure 24. - Concluded. Operational characteristics of configurations.

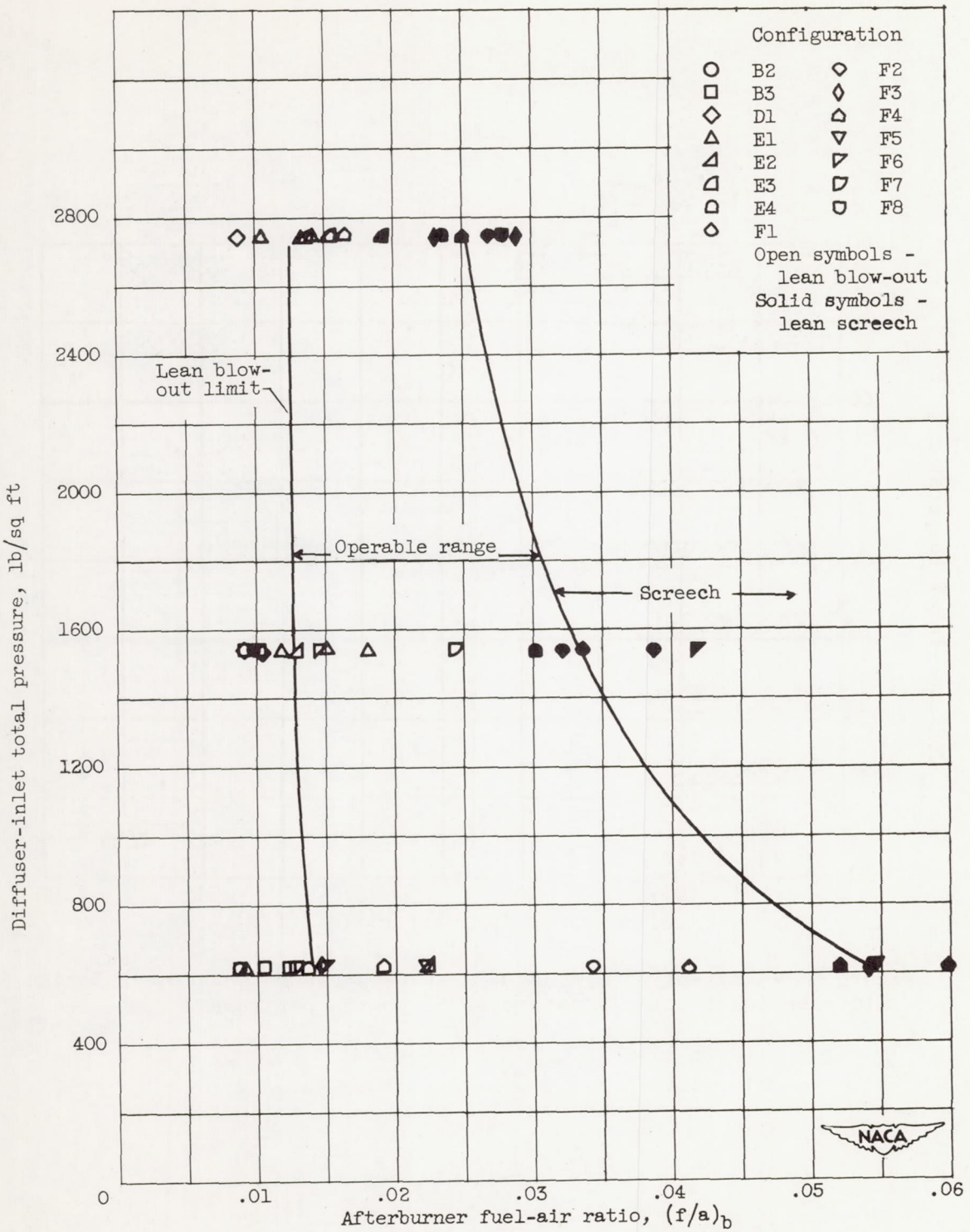

Figure 25. - Effect of diffuser-inlet total pressure and fuel-air ratio on operational limits of 15 configurations.

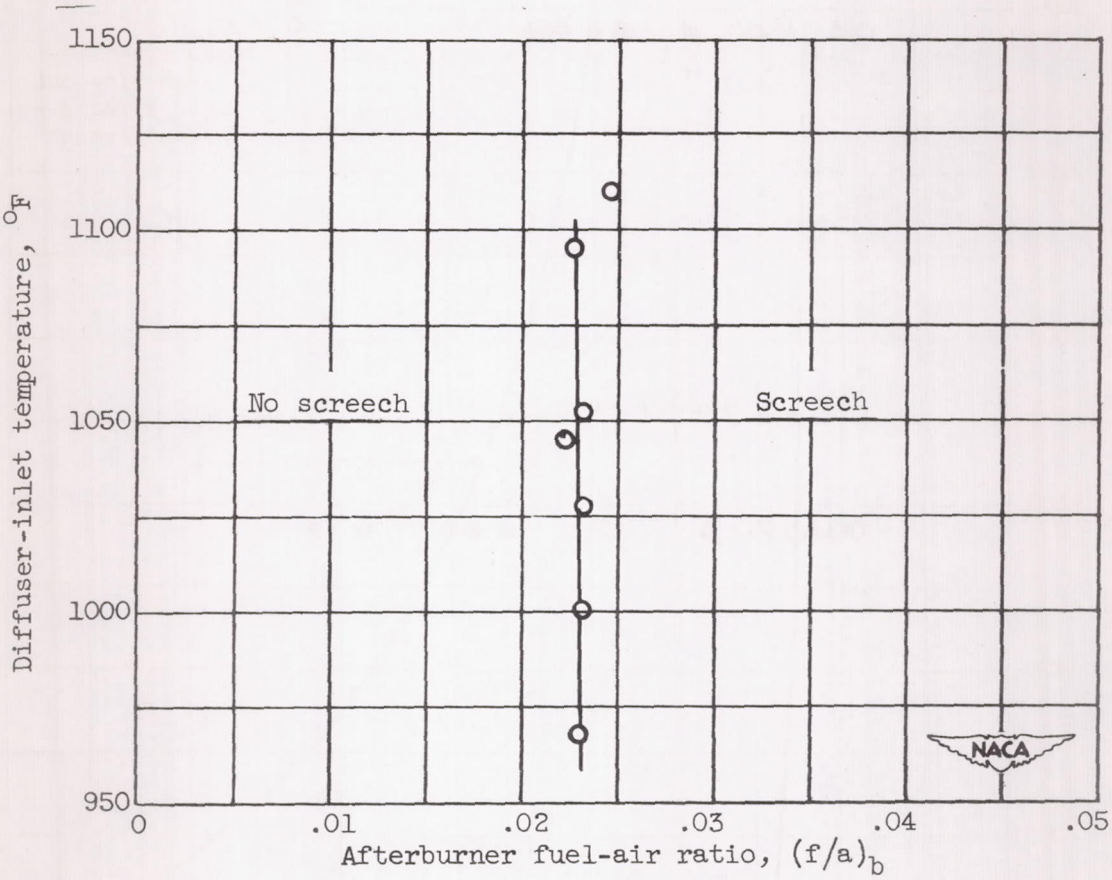

Figure 26. - Effect of diffuser-inlet temperature on screech limit. Diffuser-inlet total pressure, 2750 pounds per square foot.